Deeper Structures of Continents and Mountain Belts and Elevations

Some things below that affect things above and vice versa: Delamination will be discussed another time

ESCI 555

Elevations range from 8800 m to -11,900 m

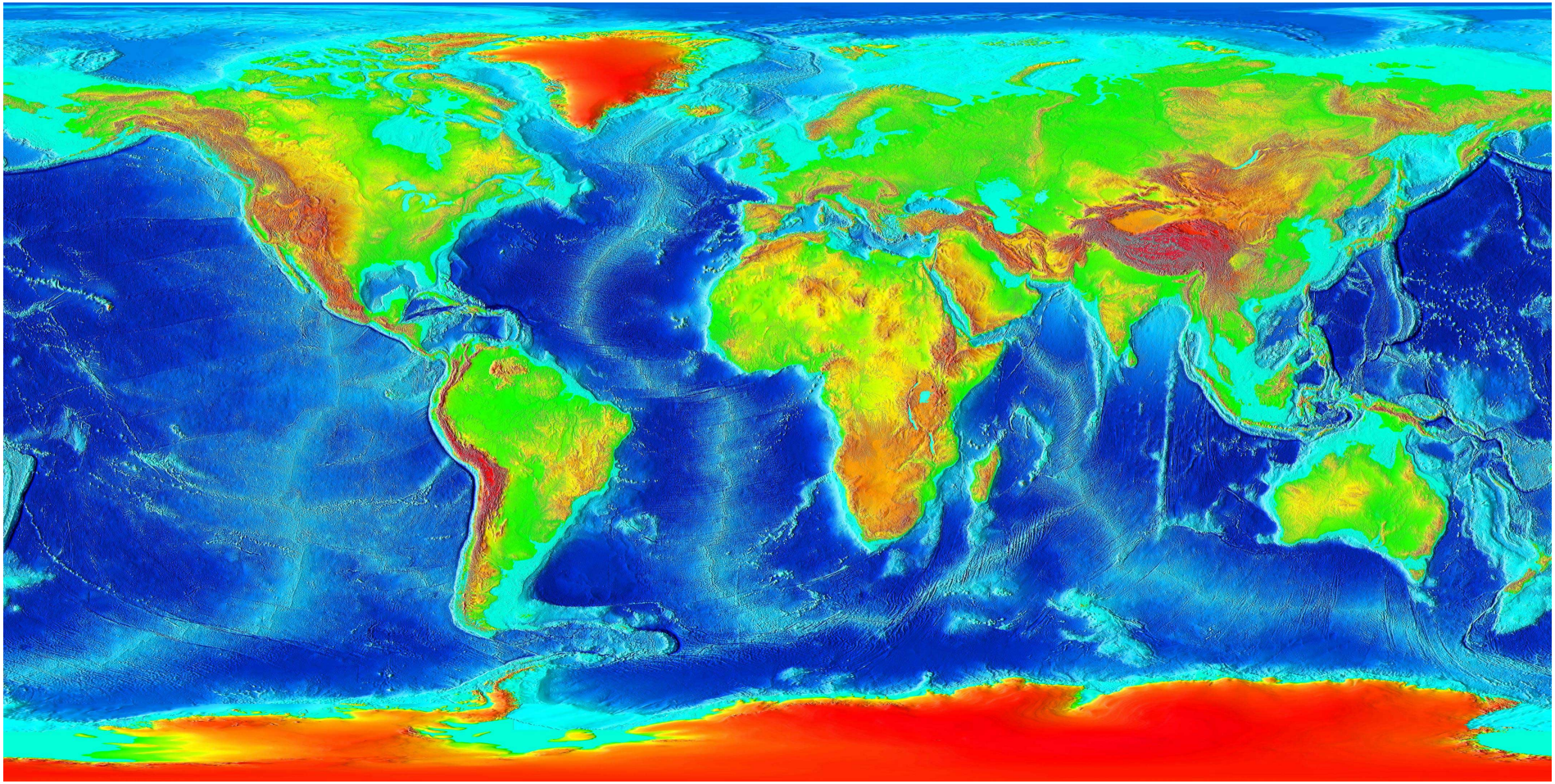

Average continental elevation is 800m

Hypsometry of Earth

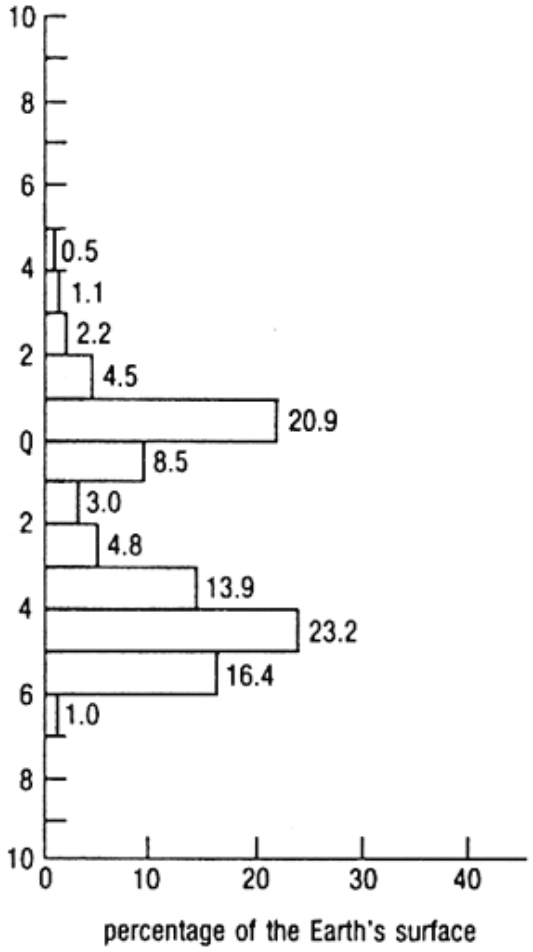

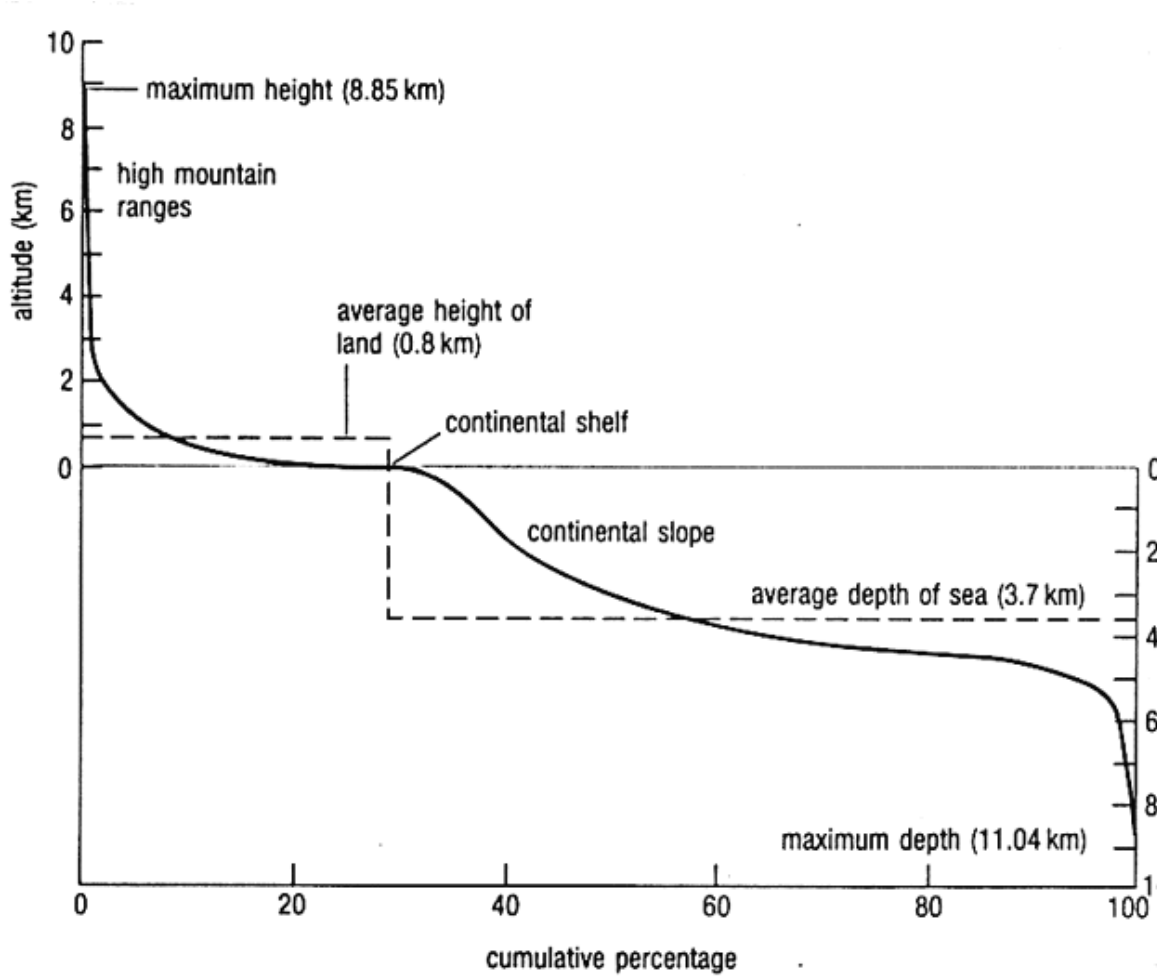

Wikipedia

Orographic Exhumation Affecting Orogenesis from Above

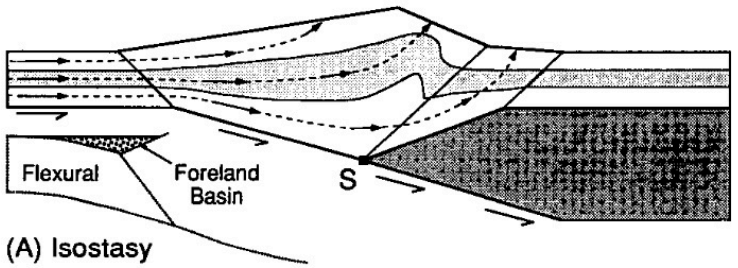

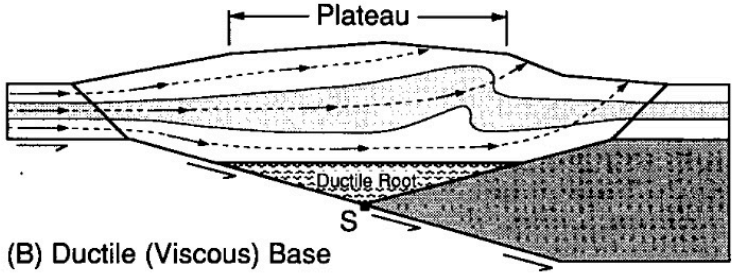

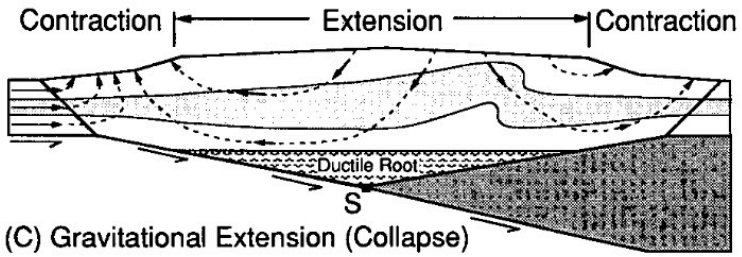

Willet et al, Geology, 1993

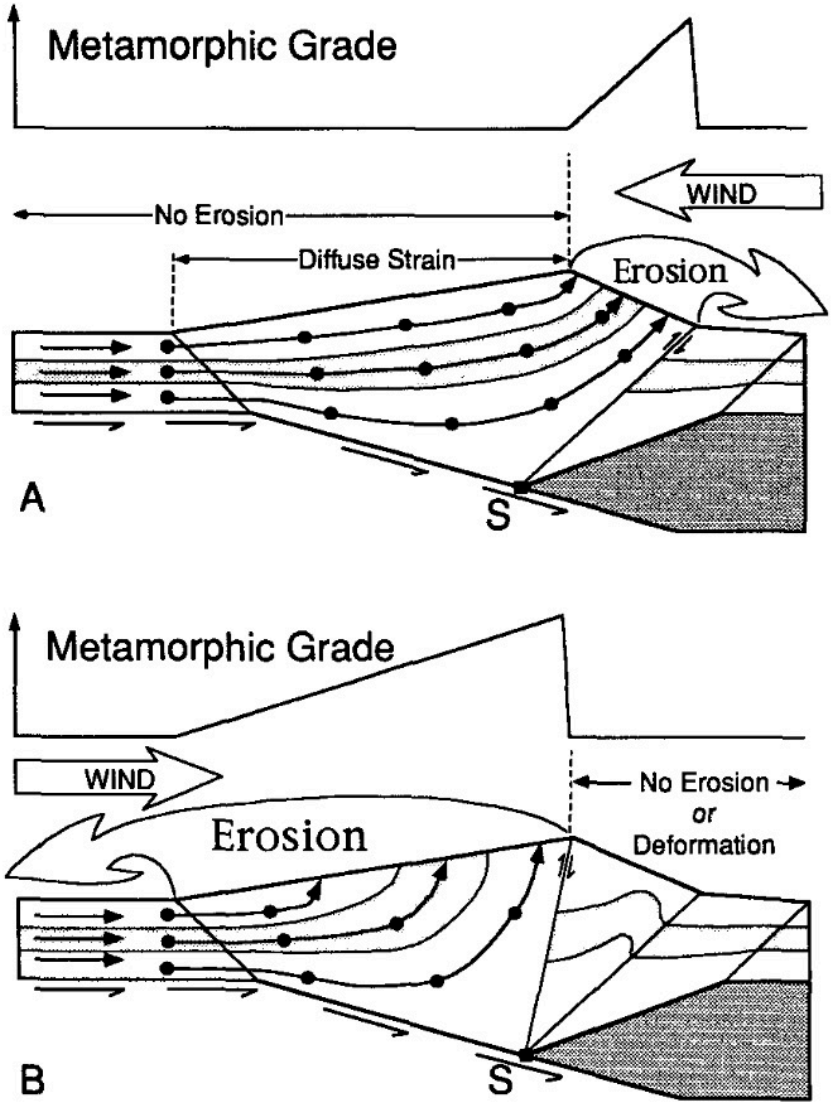

Figure 4. Effect of steady-state (constant geometry and mass) erosion and denudation. A: Retro-wedge denudation. B: Pro-wedge denudation. Passive shaded layer shows exhumed position of middle crust. Lines are material trajectories; dots are progressive equal-time positions of points initially aligned vertically. Schematic metamorphic grade is for surface rocks assuming initial equilibrium conditions.

Wind direction determines loci of exhumation of high pressure/ high strain rocks

Observed in NZ (west)
Alps (south)
Himalayas (south)
Brooks Range (south)

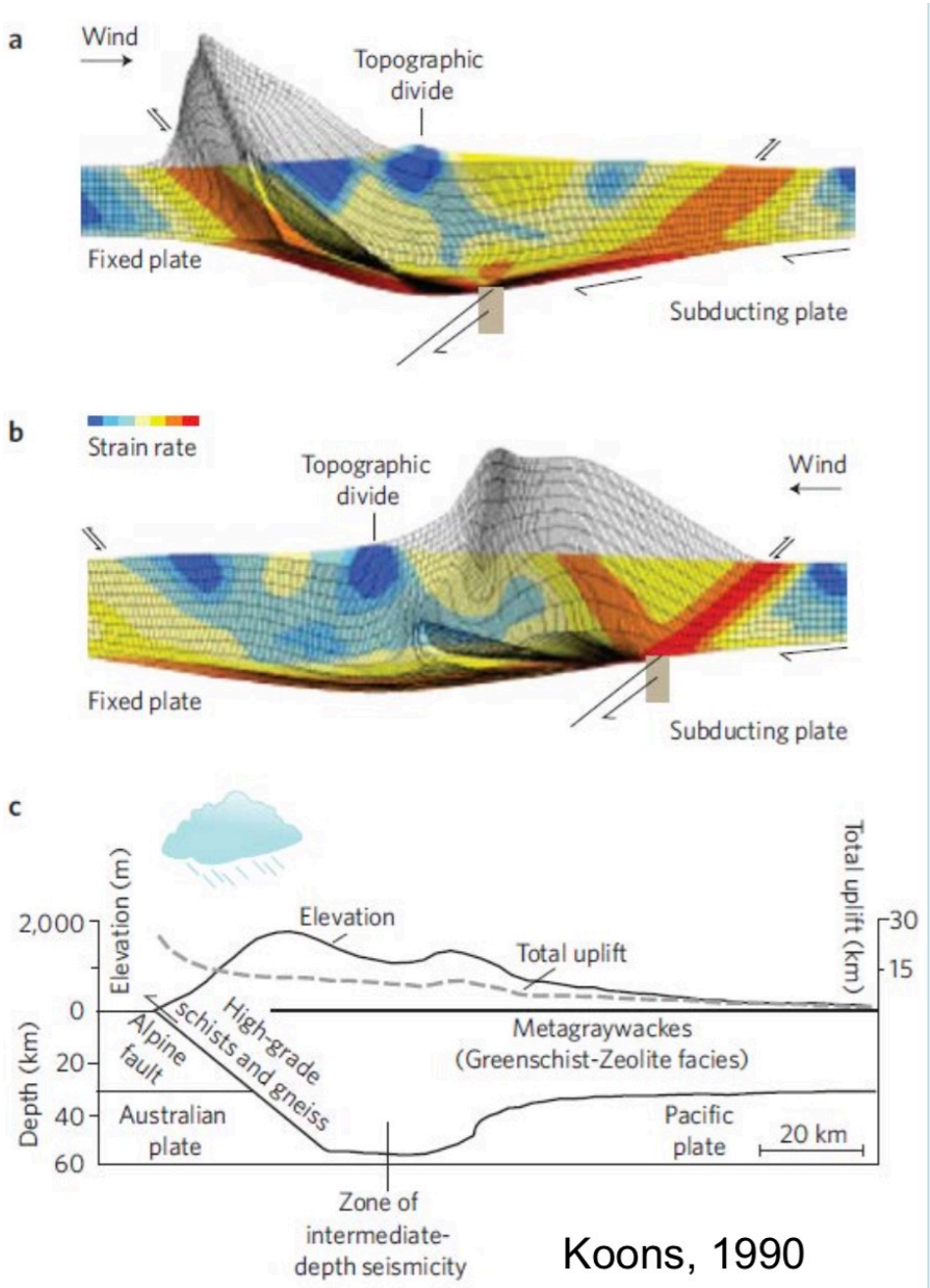

Glacial Buzz Saw: Affecting Orogenesis From Above

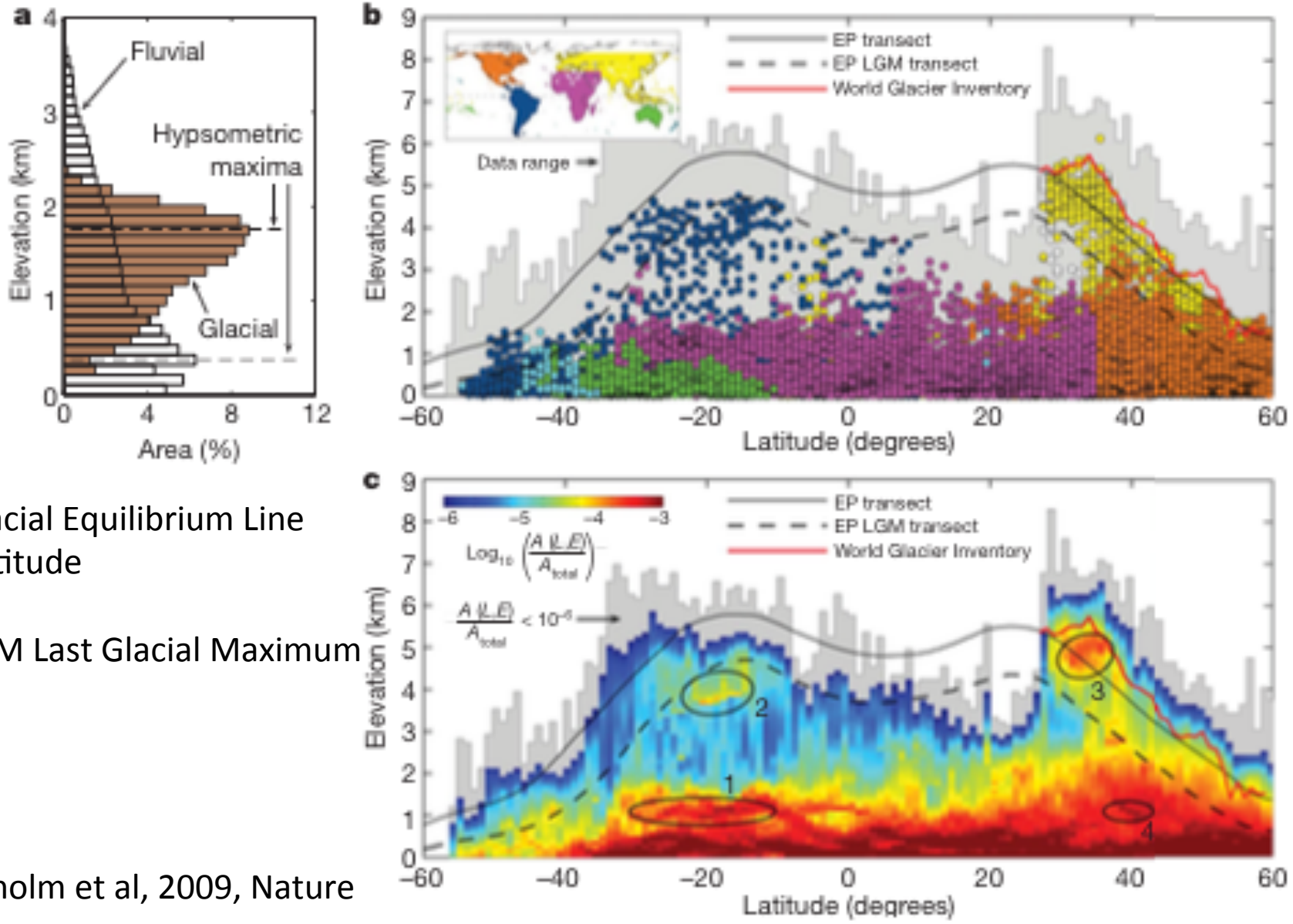

Glacial Equilibrium Line Altitude

LGM Last Glacial Maximum

Egholm et al, 2009, Nature

The Free Air Gravity

g_{FA} ~0: The earth is in isostatic equilibrium

Exceptions: Area of Laurentide ice sheet & geoid anomaly in Indian Ocean

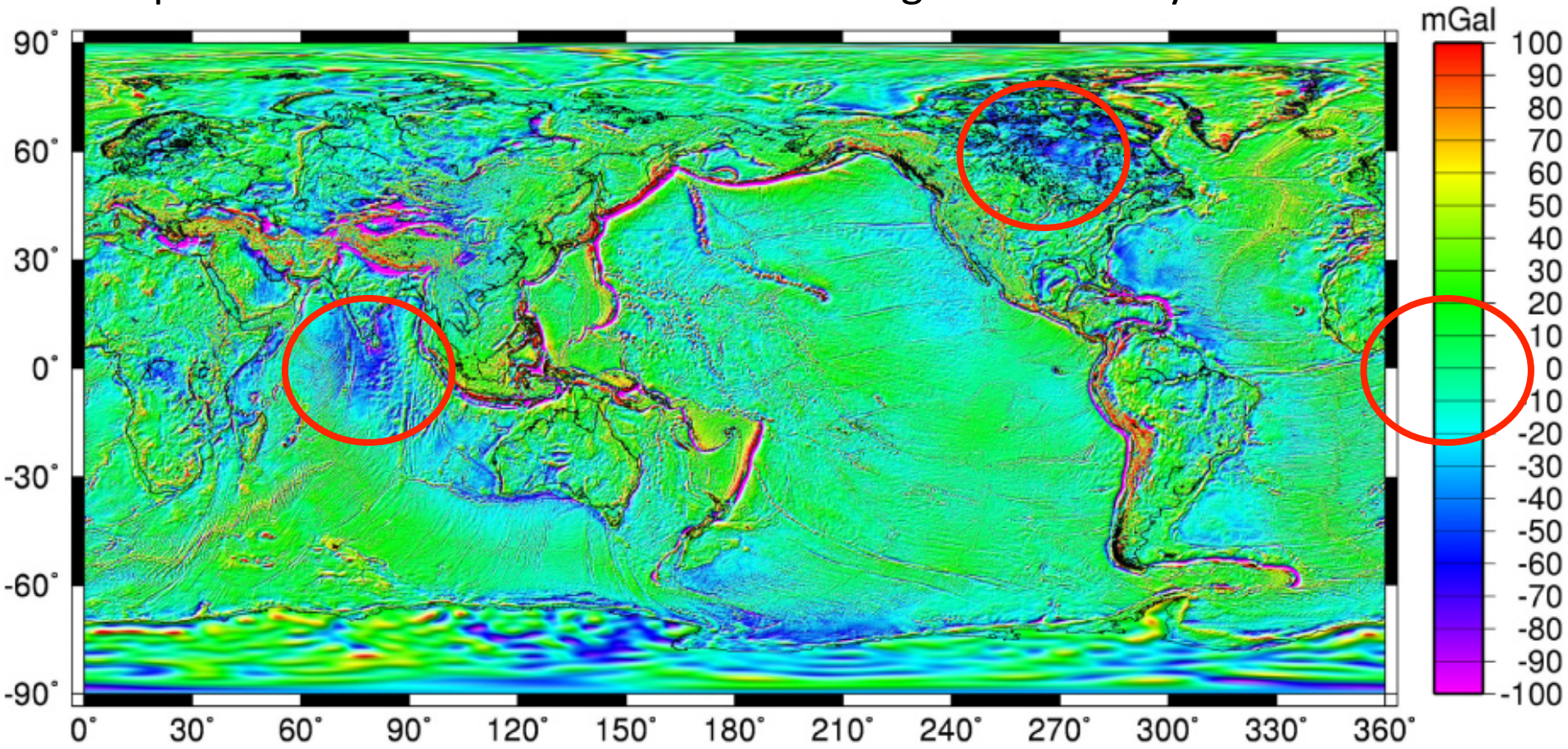

Free Air Gravity is approximately 0 over isostatically compensated regions, excluding edge effects. High frequency anomalies are edge effects between crust/lithosphere columns of different thicknesses: Indicate potential energy gradients in lithosphere

Crustal Thickness from ESA GOCE Gravity
GOCE=Gravity Ocean Climate Experiment

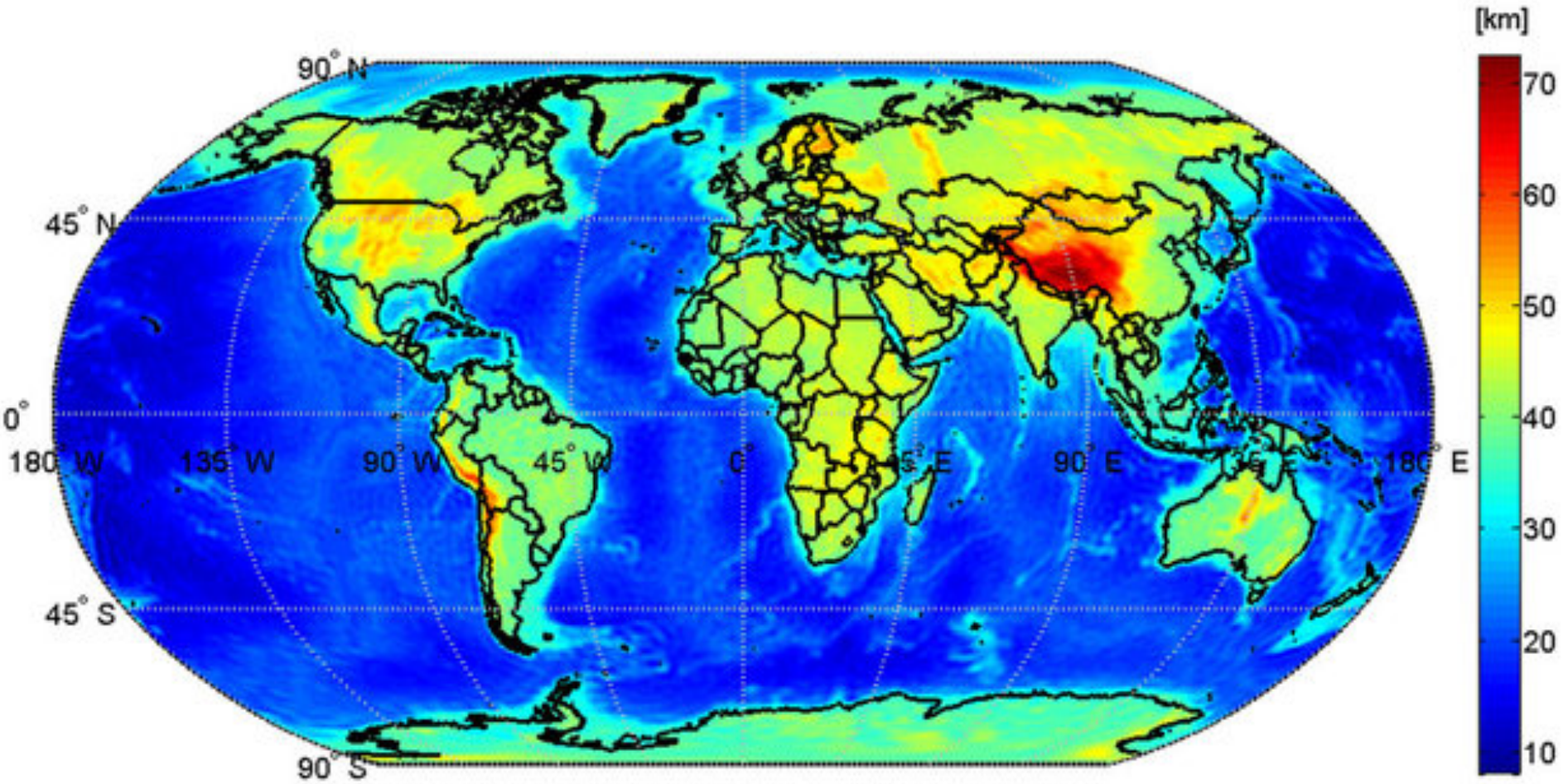

There is a strong correlation between topography and crustal thickness

Isostasy is instantaneous in comparison to other processes

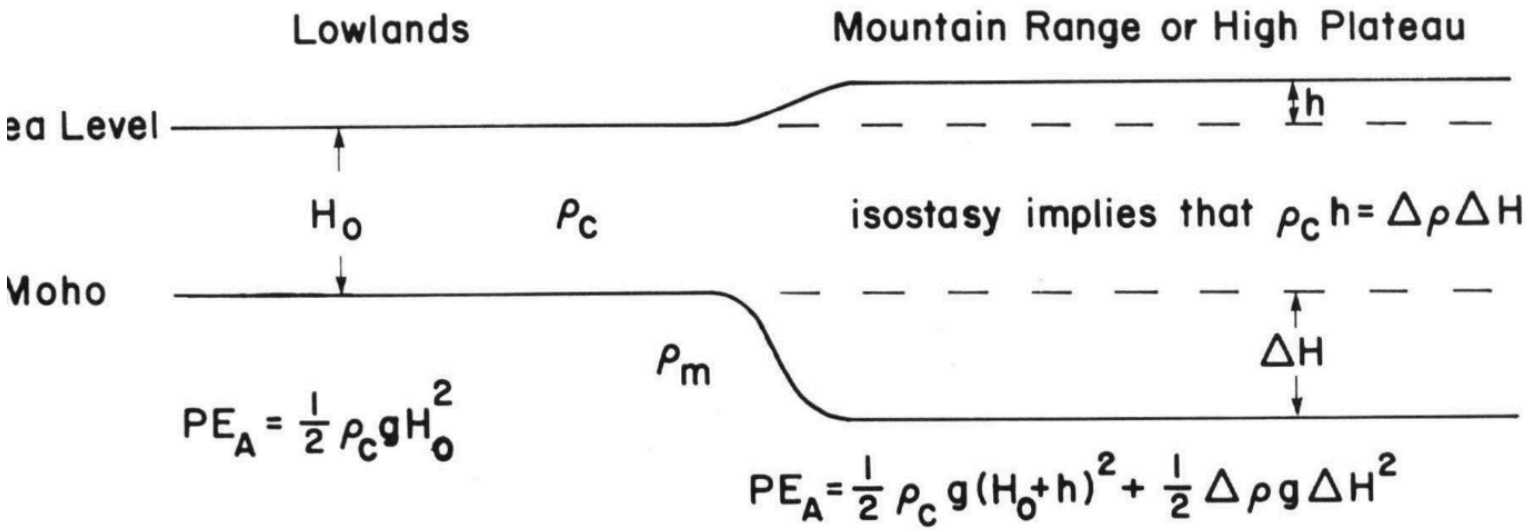

ifference between Potential Energy per unit area of Mountainous and Lowland Region

$$PE_A(\text{Mountains}) - PE_A(\text{Lowlands}) = \frac{1}{2}\rho_c g h^2 + \rho_c g H_o h + \frac{1}{2}\Delta\rho g \Delta H^2$$

$$= \rho_c g h\left(\frac{h}{2} + H_o + \frac{\Delta H}{2}\right)$$

About 2/3 of mountain belts are in Airy Isostasy

Molnar and Lyon-Caen, 1988, GSA Special Paper

Airy Isostasy: $\rho_c h = (\rho_m - \rho_c)\Delta H$

Pratt Isostasy: $\rho_c H = \rho_h (H + h)$

Isostatic Modeling including the lithospheric mantle & asthenosphere

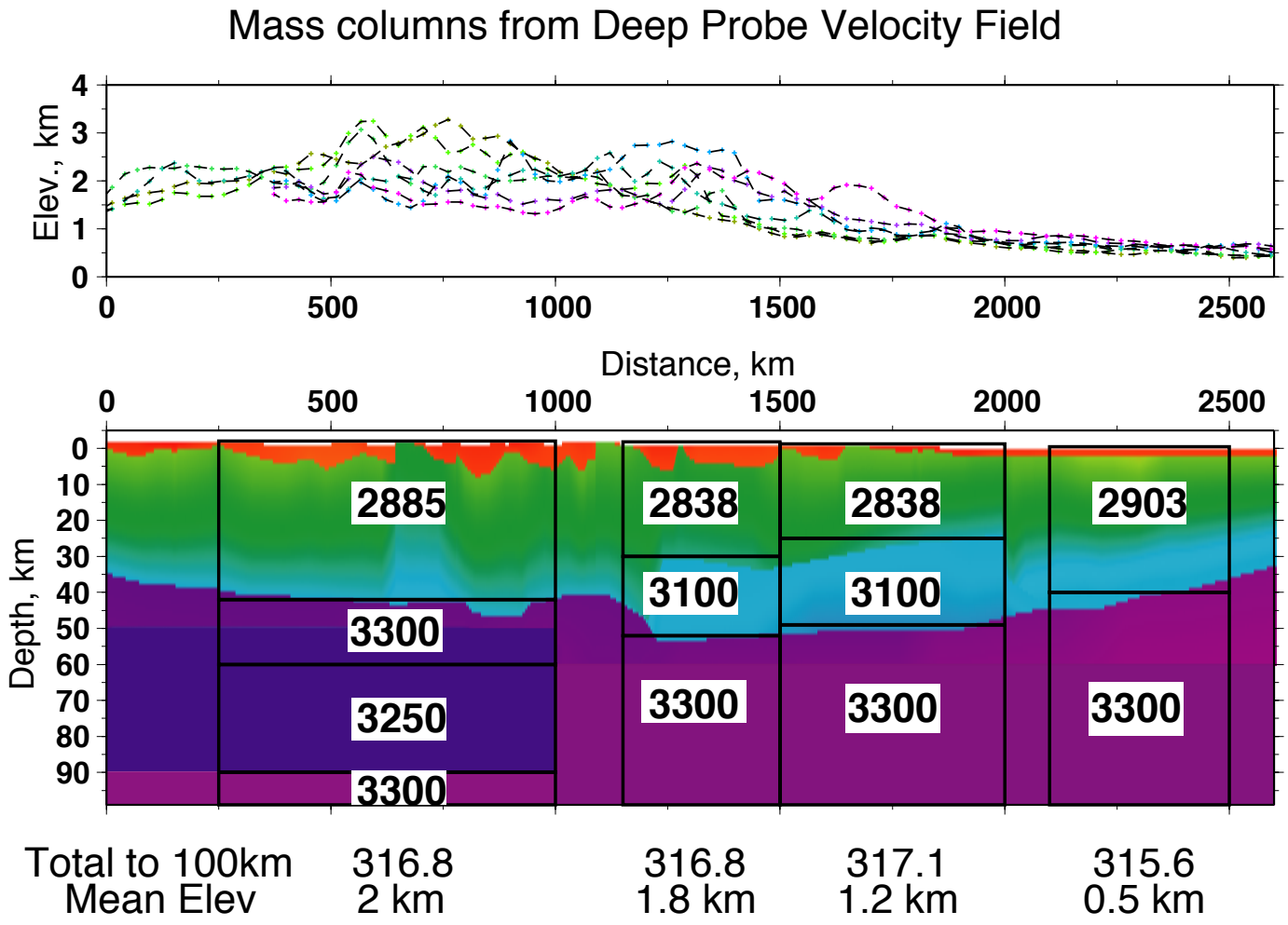

Henstock et al., 1995, GSA Today

Crustal variations are 10x more important for isostatic balance than mantle lithosphere thickness variations. (Becker et al., 2013, *EPSL*)

Local Isostasy +Regional Isostasy= Plate Flexure

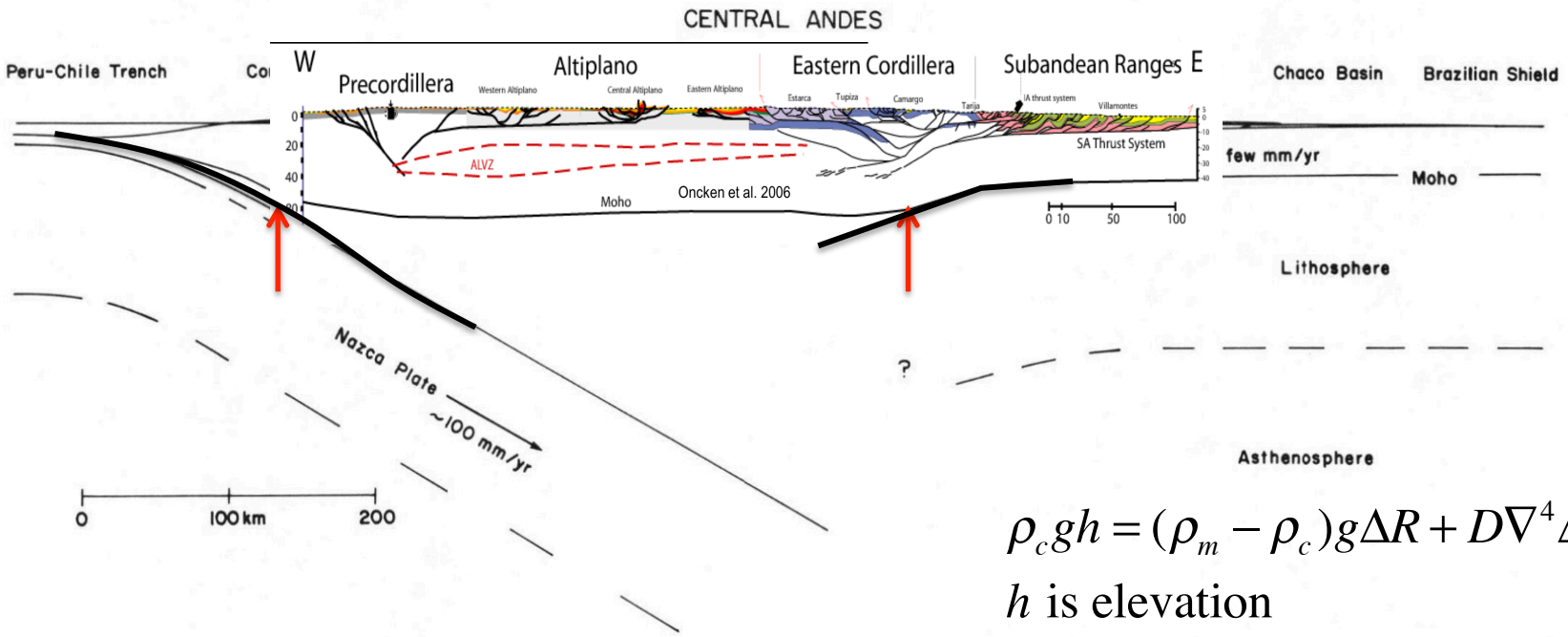

$$\lambda = \sqrt[4]{4D / g\Delta\rho}$$

$$\lambda \sim T_e^{3/4}$$

When orogenic belts exceed the strength of rocks the orogen grows laterally rather than vertically

T_e in the interior of broad plateaus is small

$$\rho_c g h = (\rho_m - \rho_c) g \Delta R + D\nabla^4 \Delta R$$

h is elevation

$\Delta R = \Delta R(x)$ is root depth

D is flexural rigidity

$\nabla^4 = \nabla^2 \nabla^2$

$$D = \frac{E T_e^3}{12(1-\sigma^2)}$$

T_e is the elastic thickness

Molnar and Lyon-Caen, 1988, GSA Special Paper

Age of
Continental Rocks

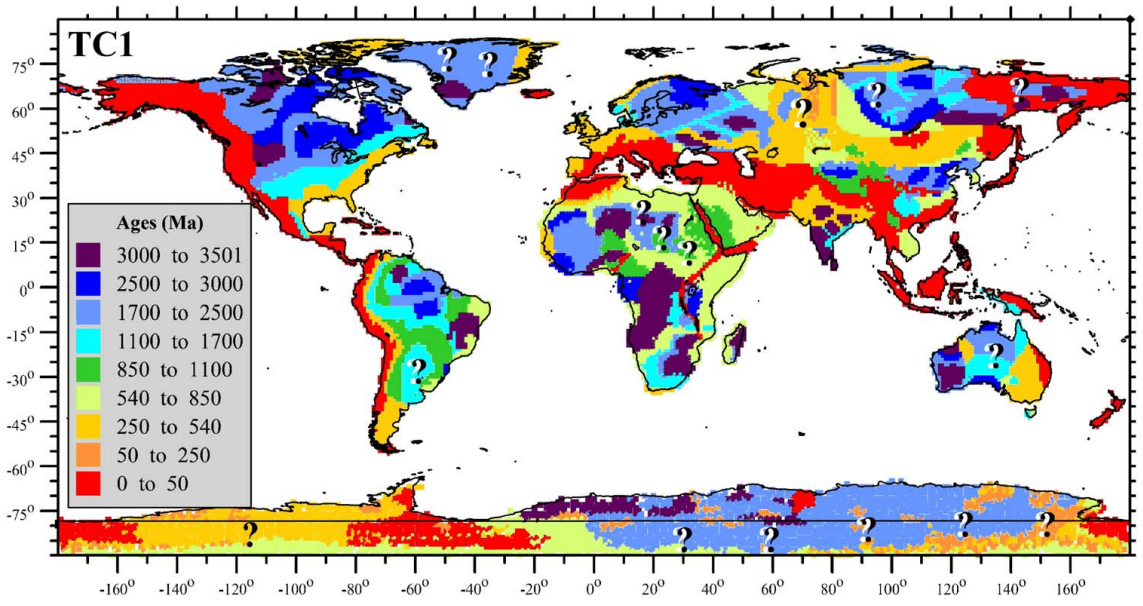

Fig. 2. Tectonic ages of the continents on a 1°×1° grid (based on Goodwin, 1996; Fitzgerald, 2002; Condie, 2005, and numerous regional publications). The map shows the ages of the major crust-forming events (see Table 1), rather than ages of the juvenile crust, and forms the basis for the global thermal model for the continental lithosphere TC1.

Lithospheric
Thickness base on
Thermal model

Artemieva, 2006,
Tectonophysics

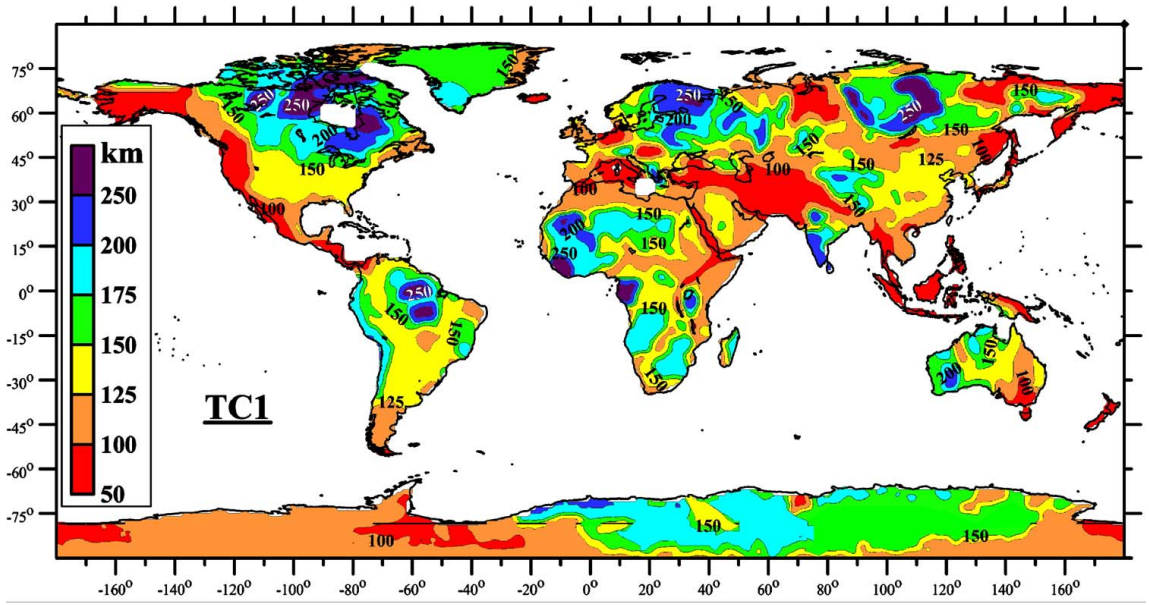

Fig. 12. Global thermal model for the continental lithosphere TC1 constrained on a 1°×1° grid: lithospheric thermal thickness interpolated with a low-pass filter. The values are based on typical continental geotherms (Figs. 3–6) and tectonic age of the basement (Fig. 2).

I.M. Artemieva / Tectonophysics 416 (2006) 245–277

Continental lithosphere thickness

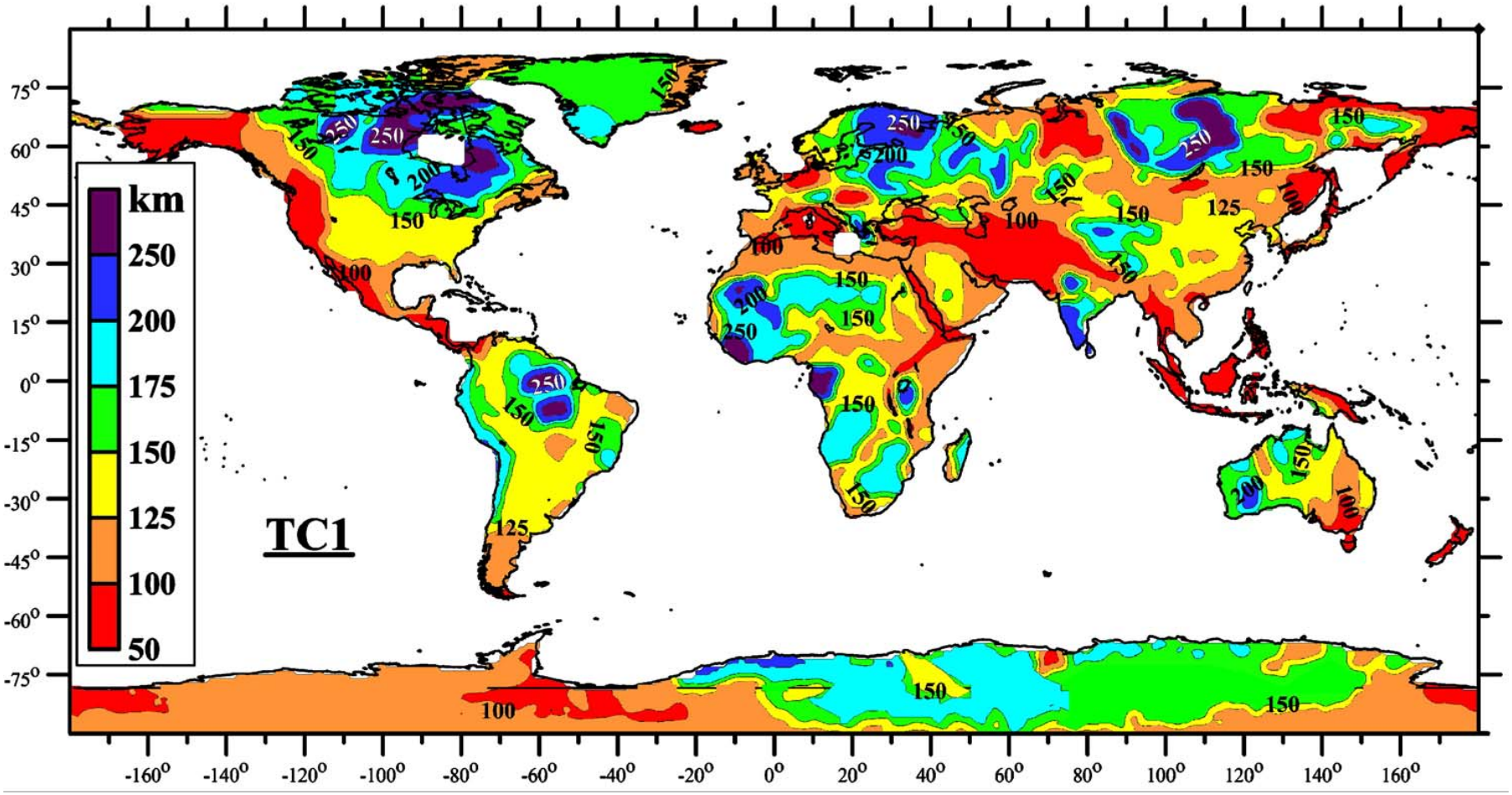

Continental Lithosphere thickness is correlated with age (although functional relationship is not as clear as oceans)

$T_e << h_{lithosphere}$ Canadian shield 40 < Te < 100 (*Audet & Mareschal, 2004, EPSL*)

Lithosphere thickness based on upper mantle shear velocity

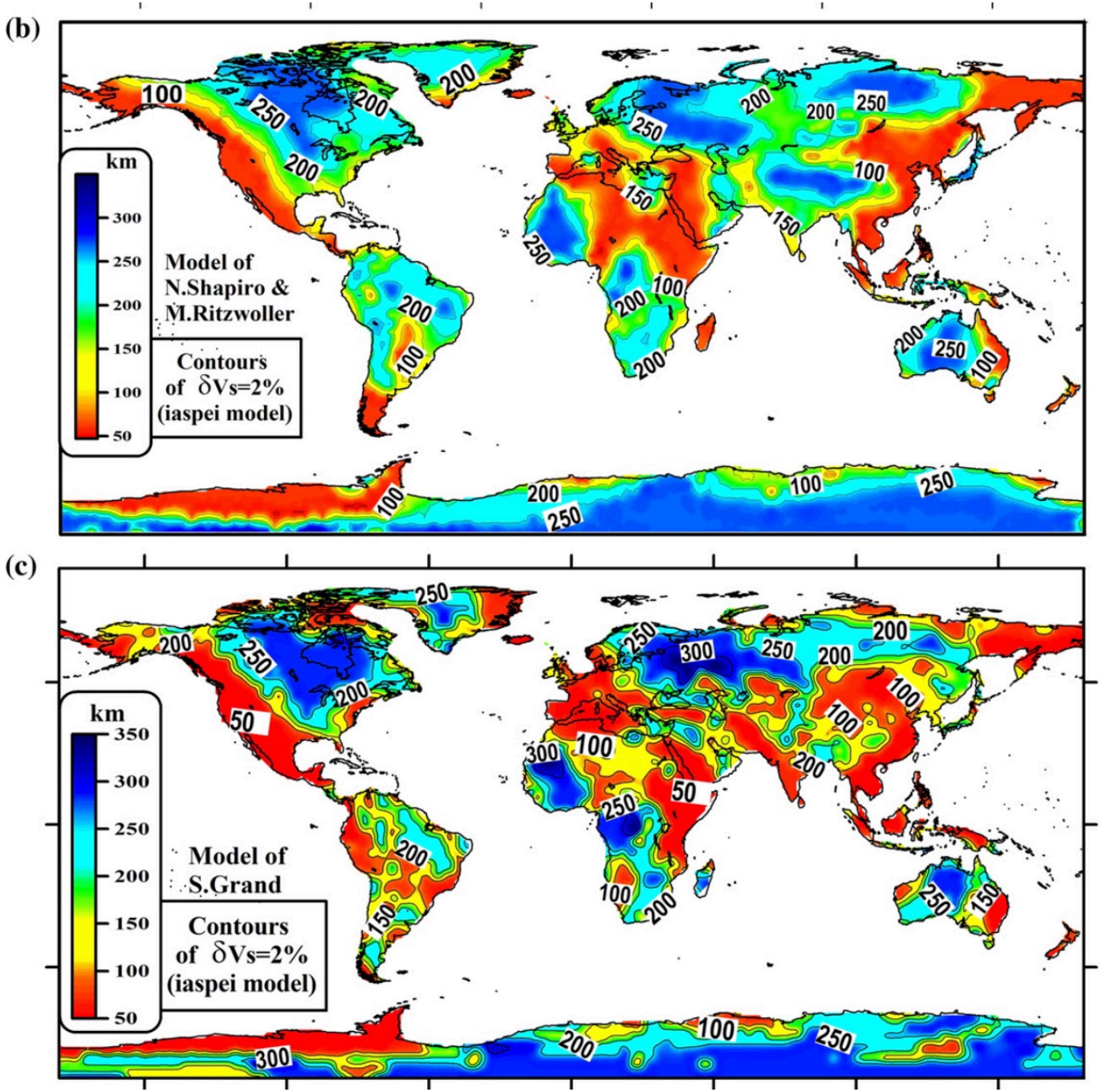

Artemieva, 2009, Lithos

US Cordillera Lithospheric Thickness

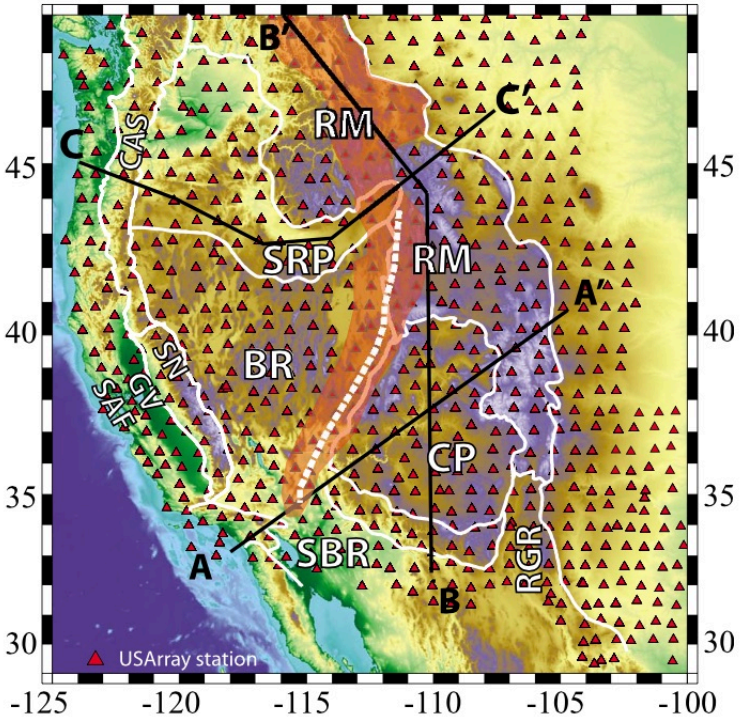

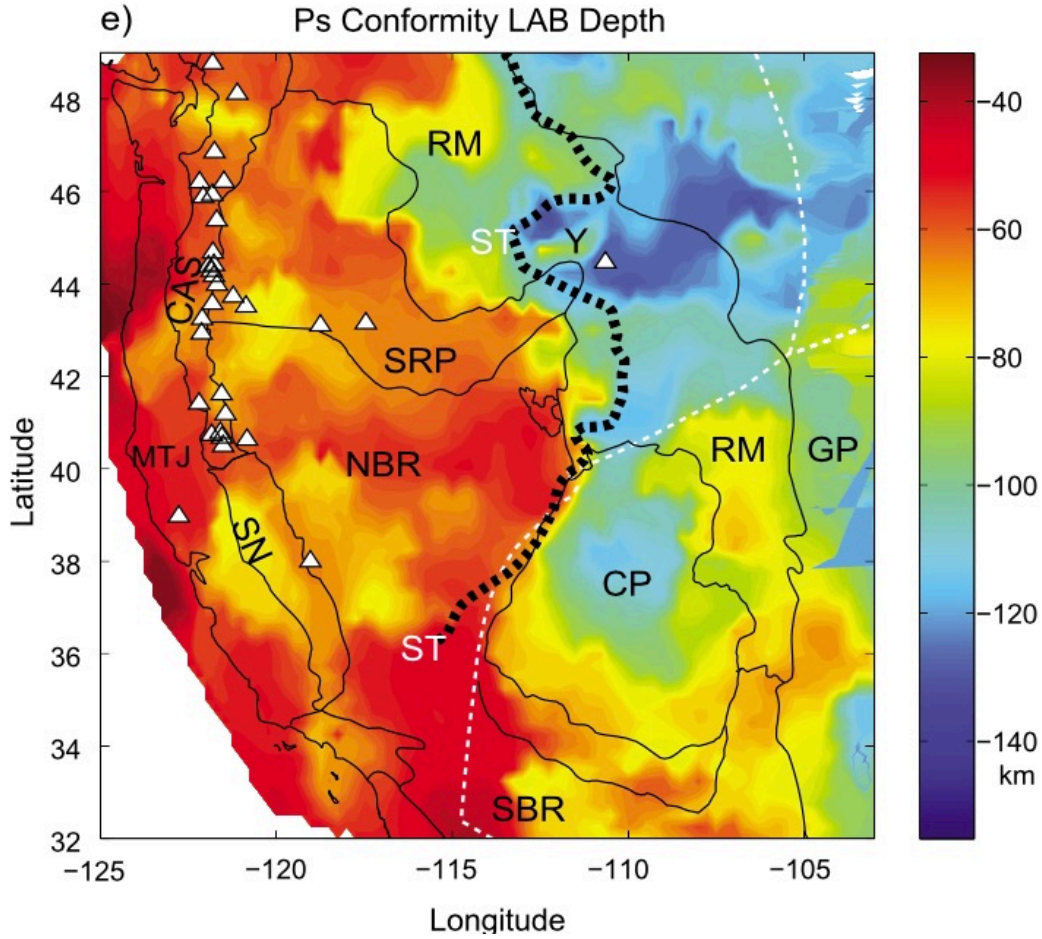

Dashed line is approximate Cordillera hingeline: Front of the Fold and thrust belt

Effective Elastic Thickness of Western US Lithosphere

Elastic Thickness is less than crustal thickness in high heat flow regions of the west

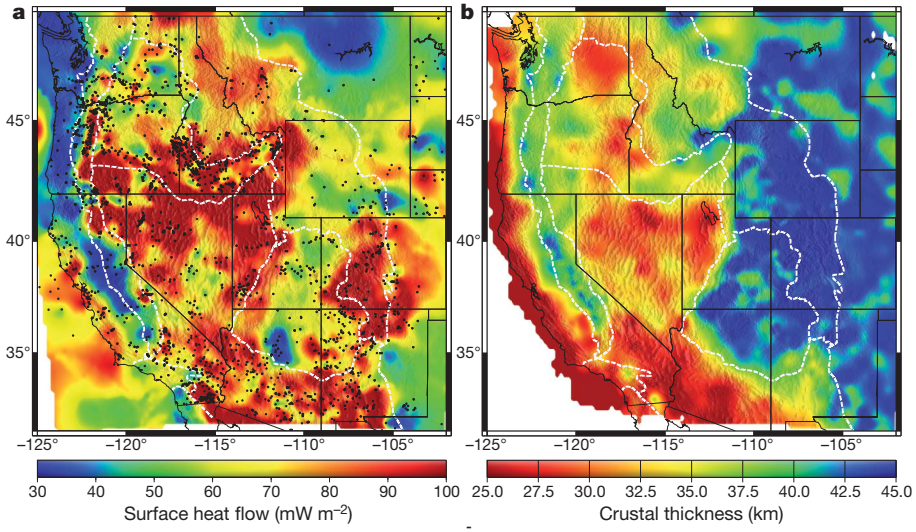

Lowry and Perez-Gussinye, 2011, Nature

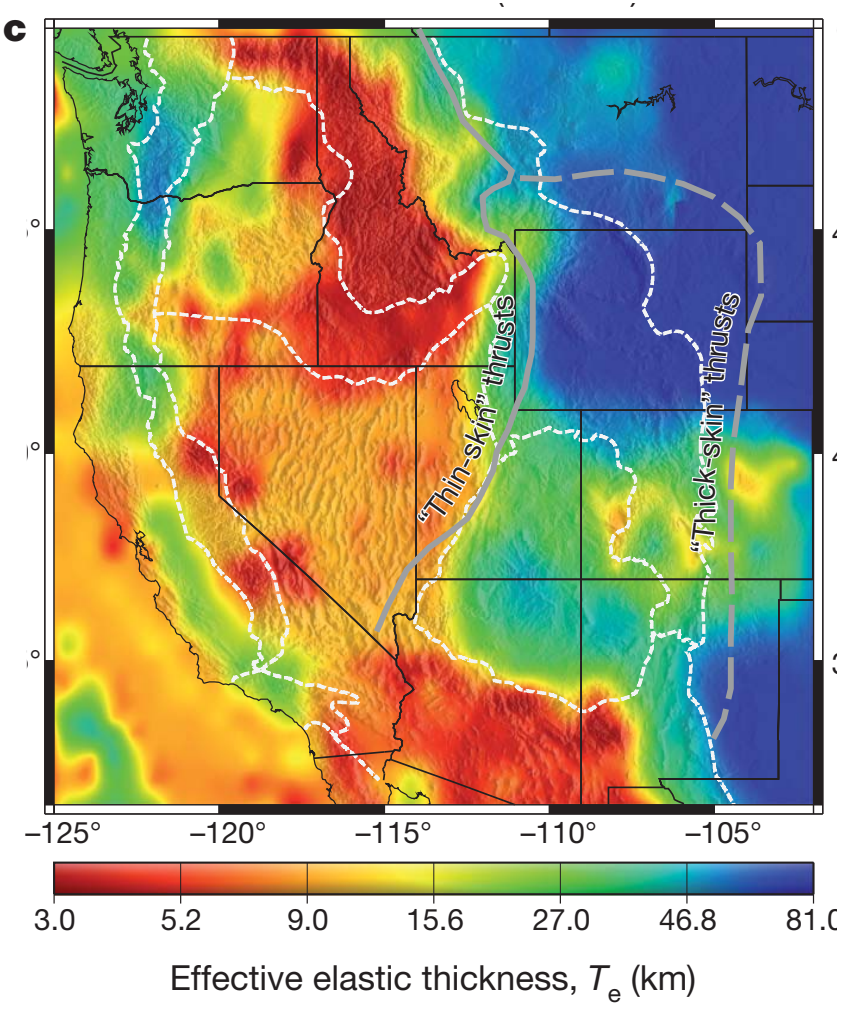

T_e under orogenic plateaus is often near 0

Lithosphere thickness based on upper mantle shear velocity

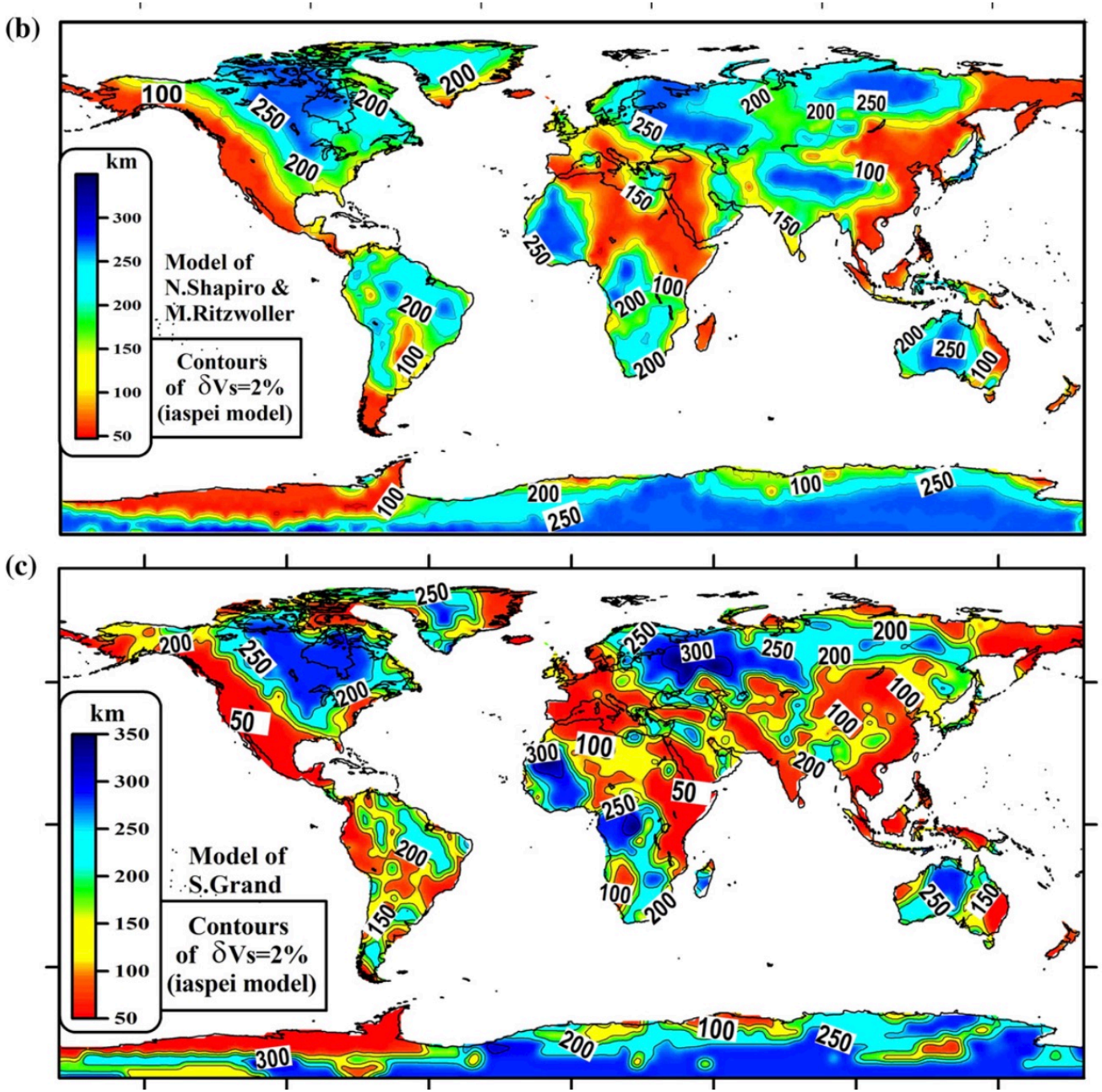

Artemieva, 2009, Lithos

Lithosphere Thickness

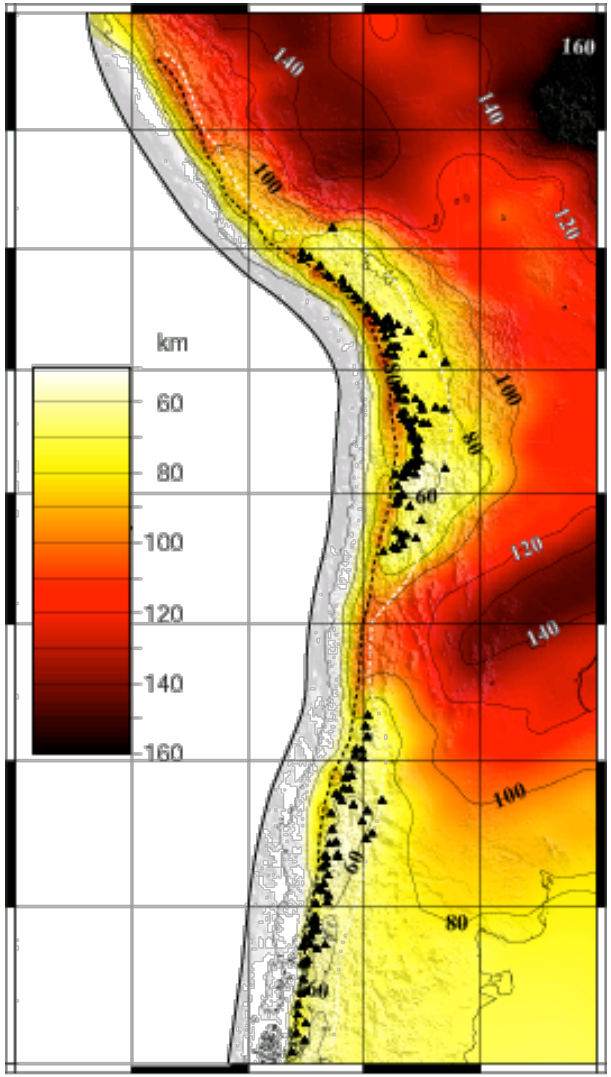

Crustal Thickness

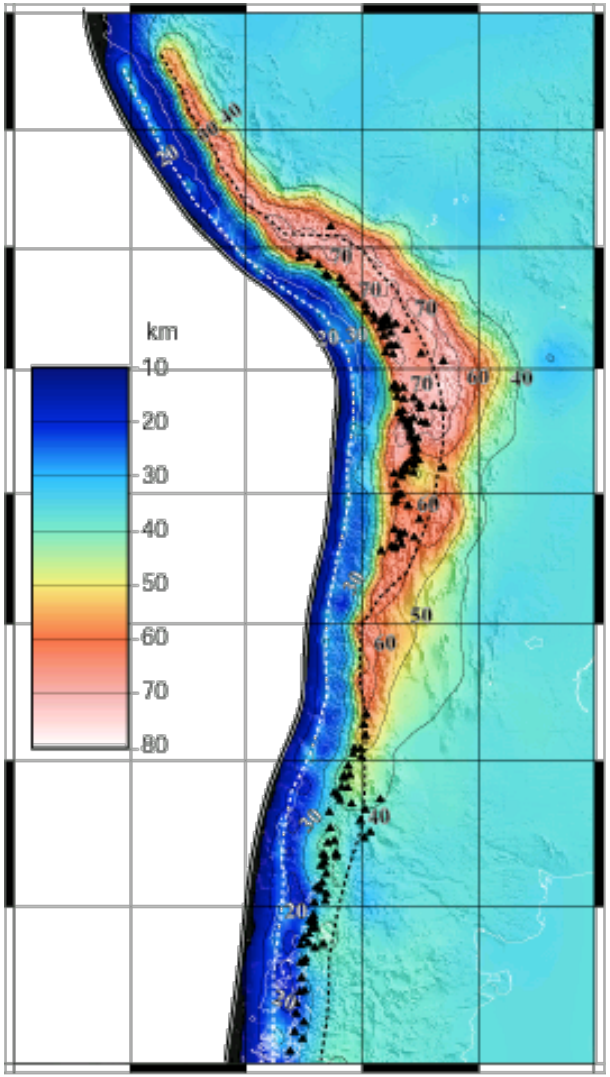

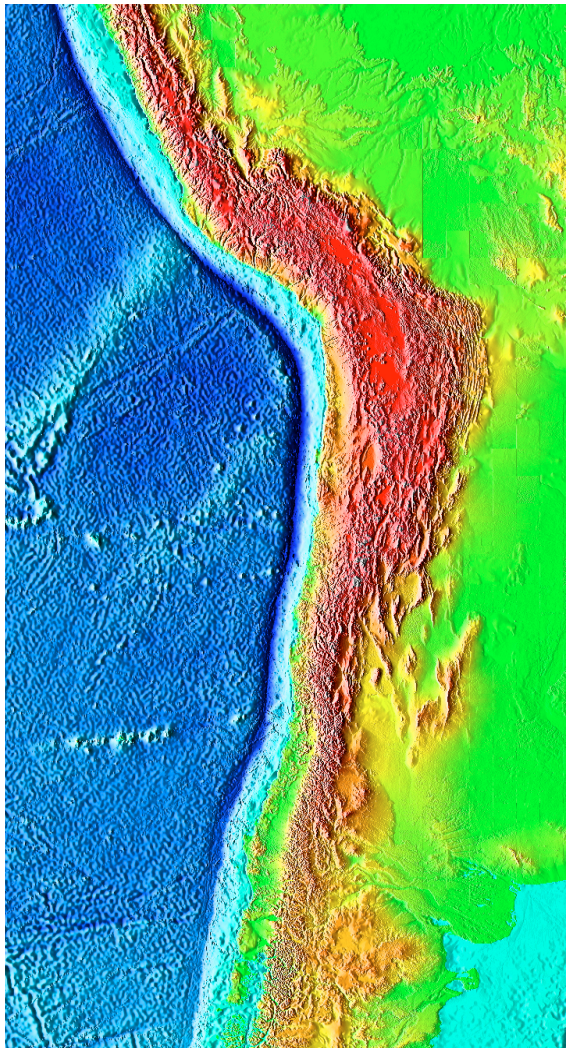

Lithosphere thickness under Altiplano is ~ crustal thickness

Lithosphere thickness based on upper mantle shear velocity

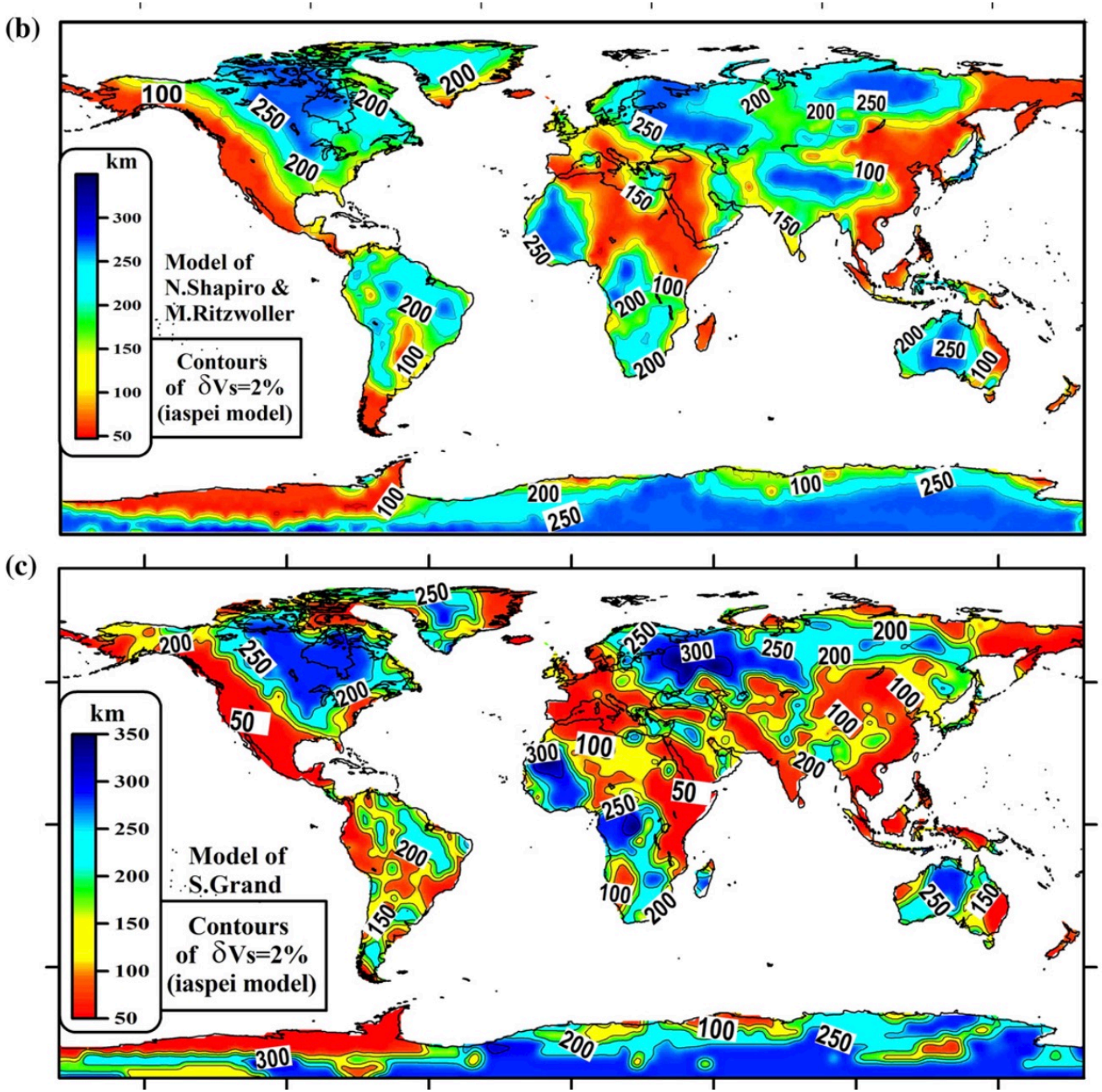

Artemieva, 2009, Lithos

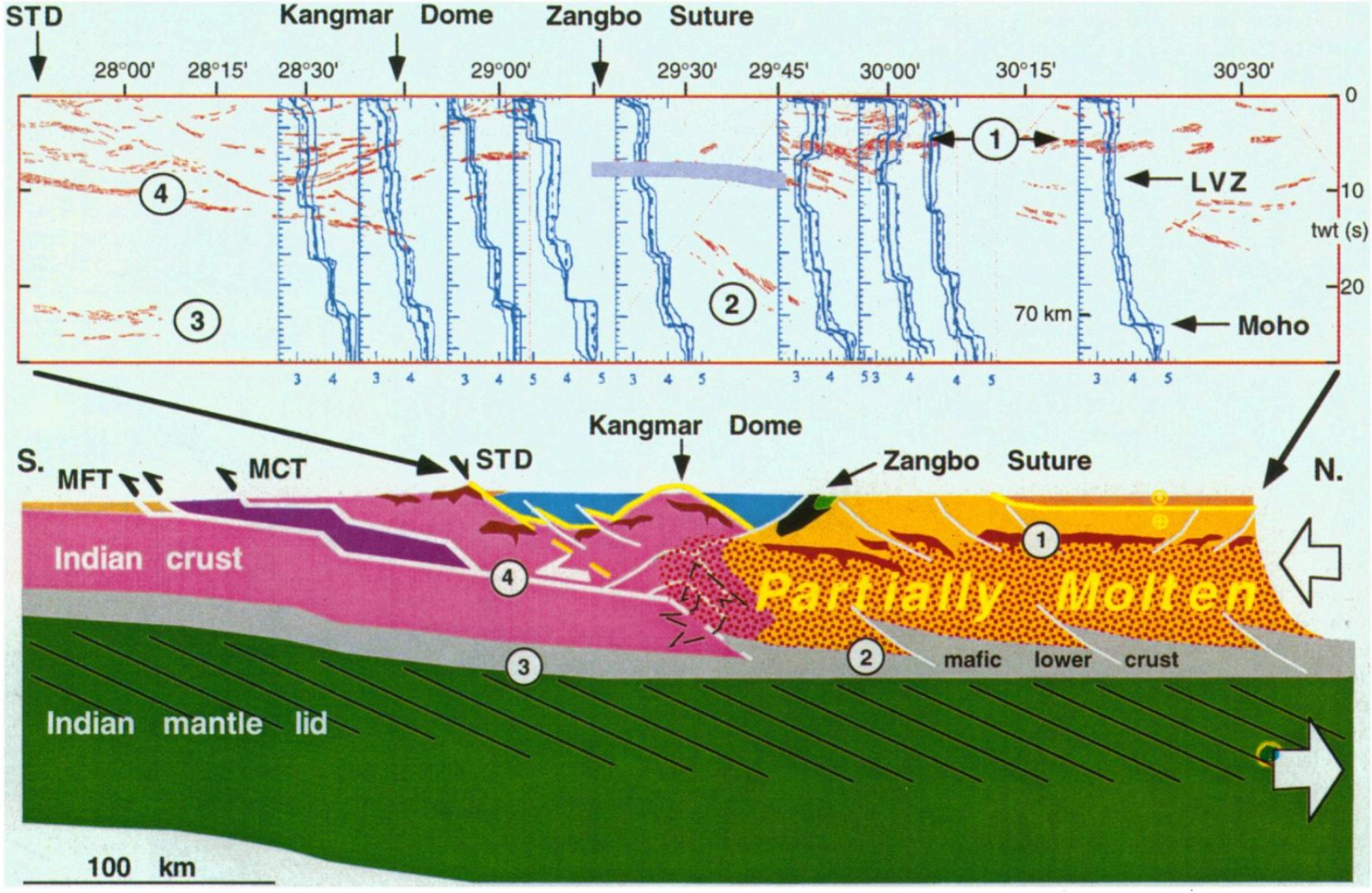

Fig. 2. (**Top**) Composite of selected INDEPTH geophysical observations along the Yadong-Gulu rift in southern Tibet; red, composite north-south CMP profile described in (*6*); blue, one-dimensional shear-wave velocity profiles derived from broadband earthquake data (*7*); blue stipple, wide-angle reflection observed in CMP data gap beneath and just north of the Zangbo suture; LVZ, midcrustal low-velocity zone evident in shear-wave velocity profiles north of the Zangbo suture. (**Bottom**) Interpretive lithosphere-scale cross-section of the Himalayan collision zone (see text). MFT, Main Frontal thrust; MCT, Main Central thrust; STD, South Tibetan detachment system. Numbers refer to features discussed in text.

Himalyan Front: Erosion redirects channel flow

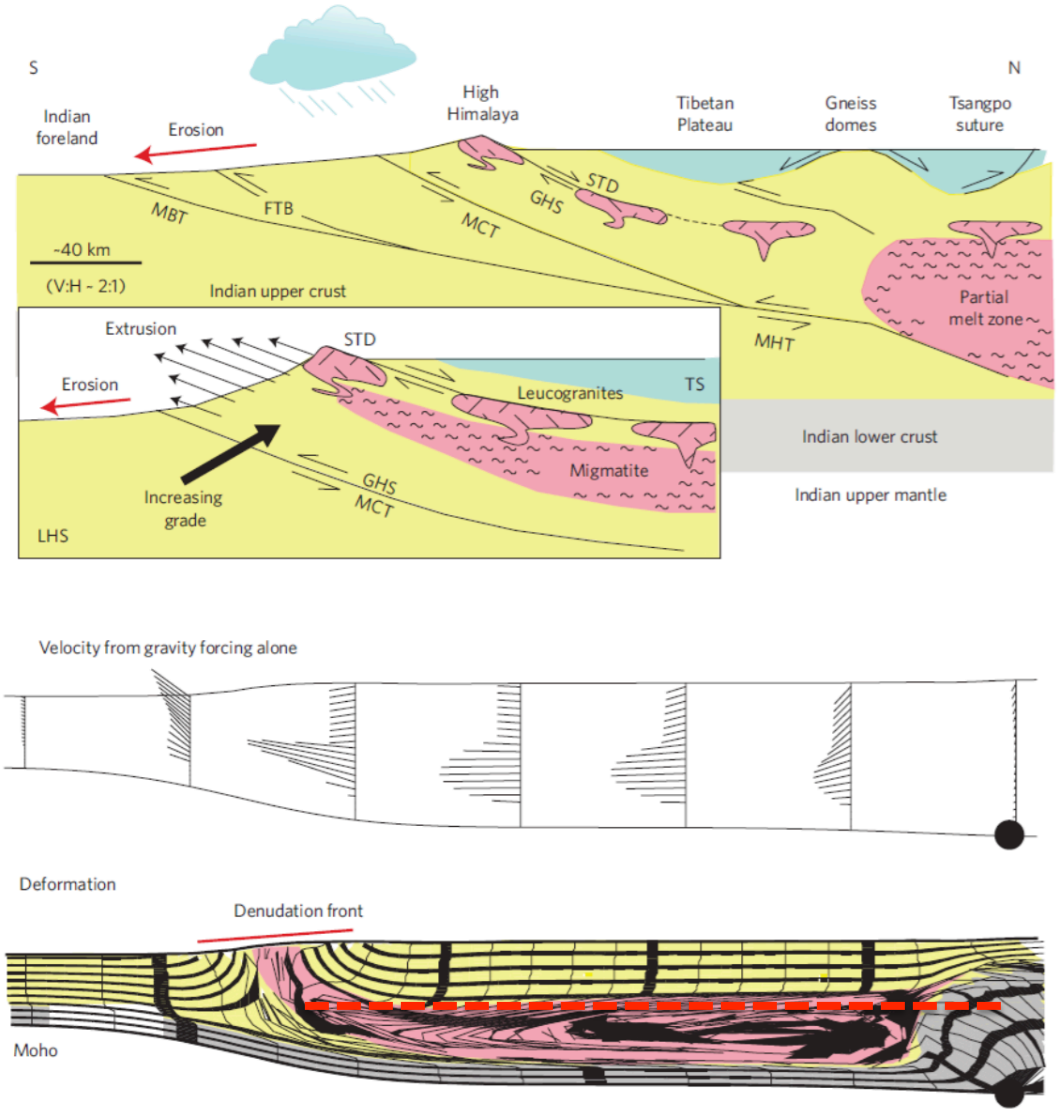

Channel flow and exhumation in Tibet and Himalayas driven by erosion

Beaumont et al., 2001

Himalayan Support from Plate Flexure

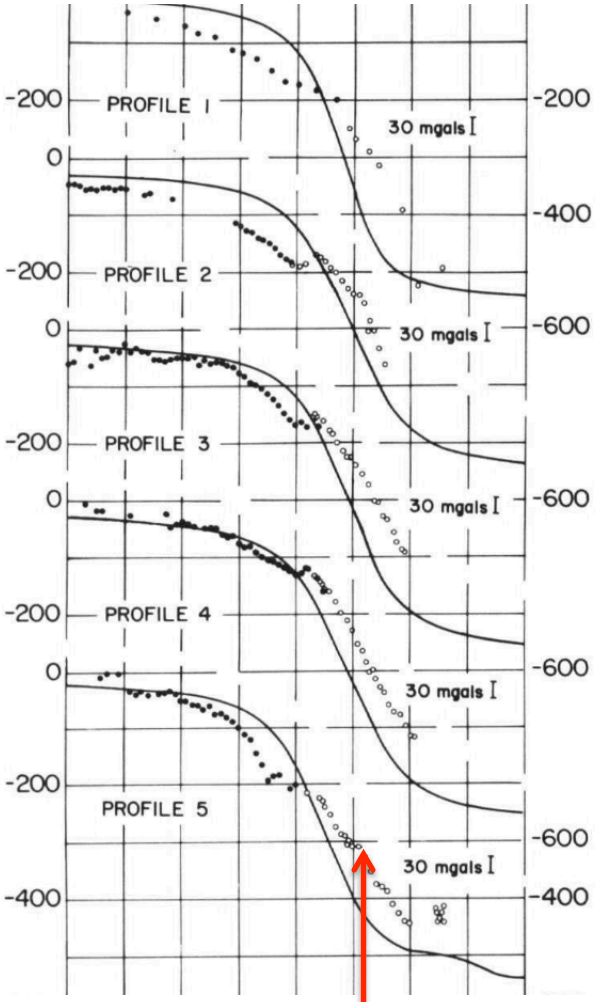

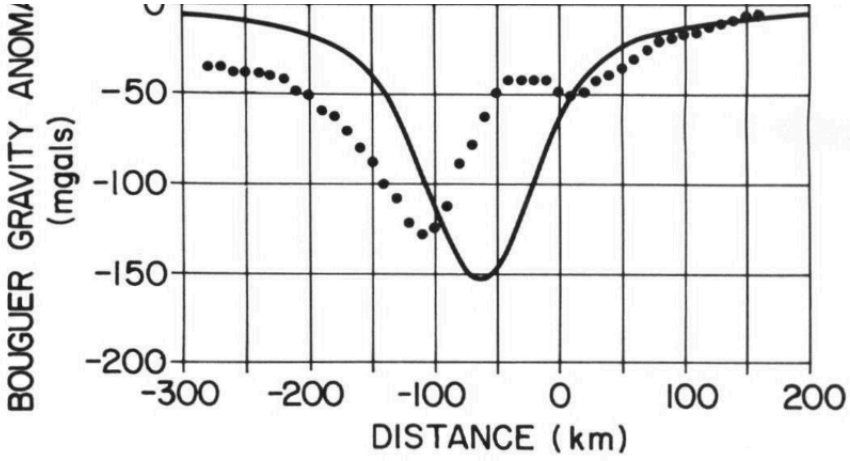

Figure 4. Comparisons of measured Bouguer gravity anomalies and those calculated assuming local isostatic compensation. (a) Five profiles across the Himalaya (from Lyon-Caen and Molnar, 1985). Closed circles represent points taken from the listing compiled by the Defense Mapping Agency; open circles represent points from Kono (1974) for profile 1 and from Das and others (1979) for the other profiles. Note the more negative observed values over the Ganga basin, which reflect a deficit of mass there, and the less negative observed values over the Lesser Himalaya, which reflect an excess mass there. (b) One profile across the Venezuelan Andes. Data are from Bowin (1976), Folinsbee (1972), and Bonini and others (1977), and calculations are by R. Benites and others (in preparation). As for the Himalaya, note the more negative observed values over the basins and the less negative values over the mountains. Again, the flexed plates beneath the basins are filled with low-density sediments, while the strength of the plates redistributes the support of the

Results from flexural support

Lithosphere under Southern Tibetan Plateau

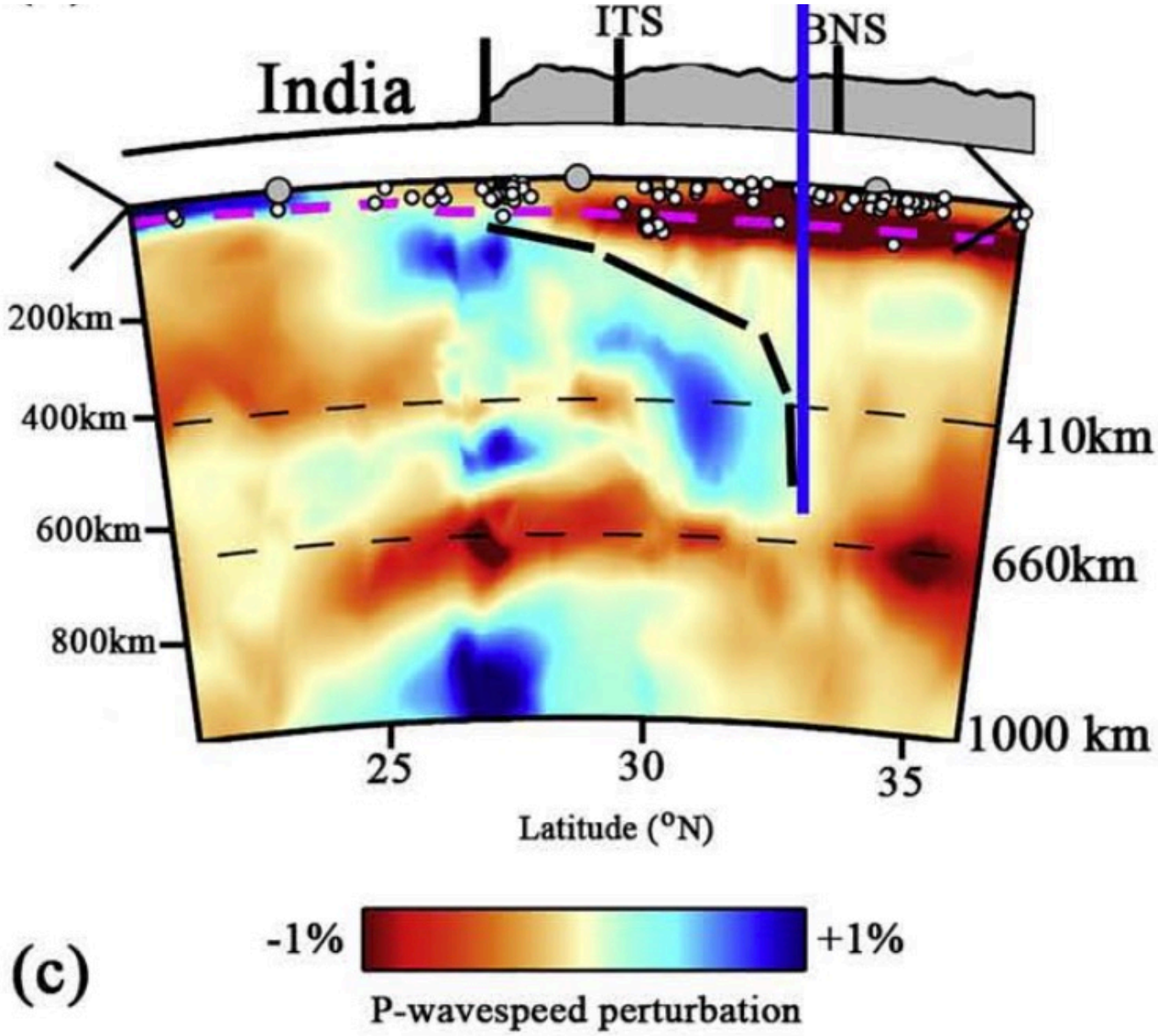

Chang et al, 2008 EPSL

Global prevalence of the glacial buzzsaw.

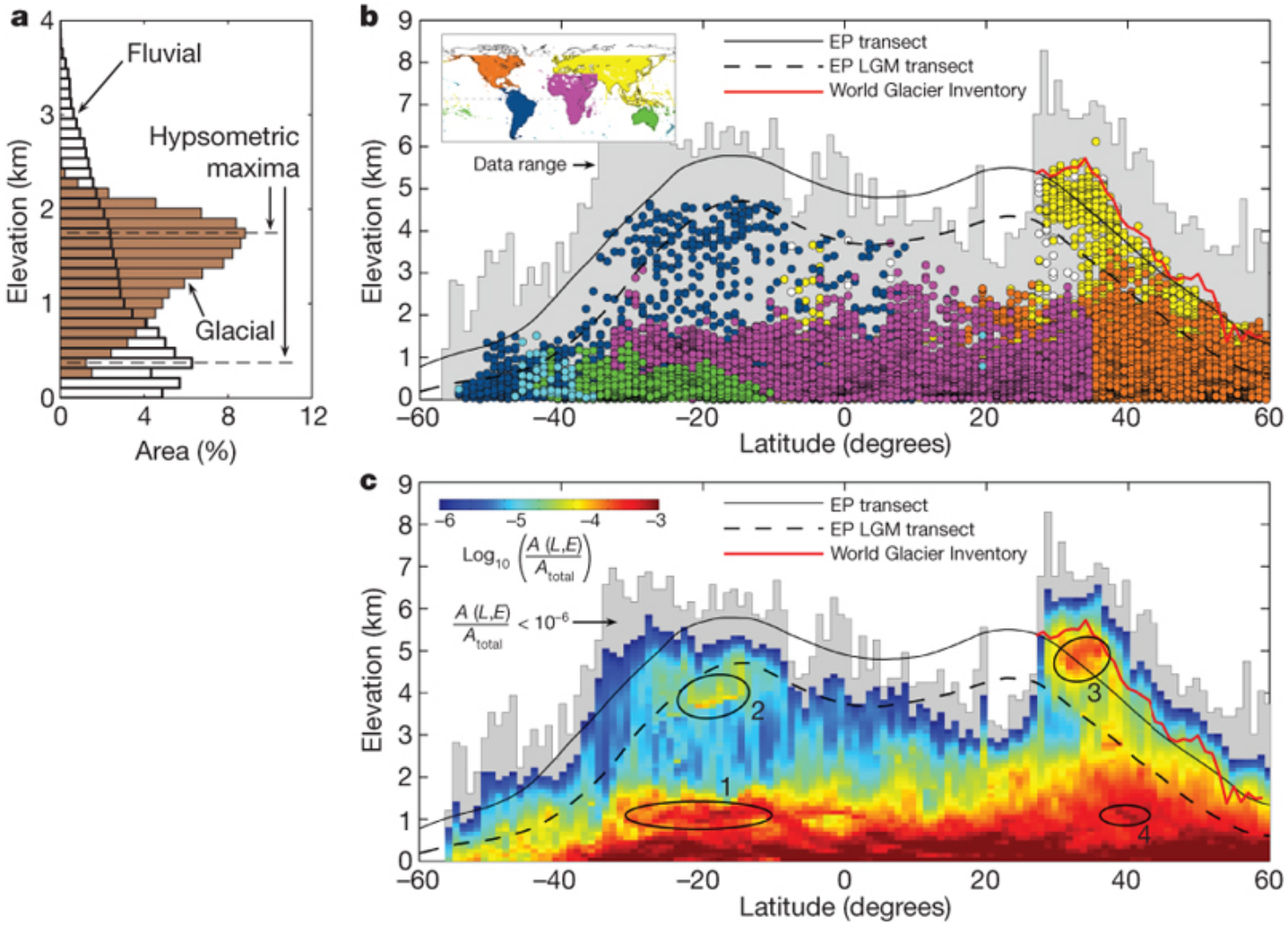

nature

DL Egholm *et al. Nature* **460**, 884-887 (2009) doi:10.1038/nature08263

Complete Bouguer Anomaly

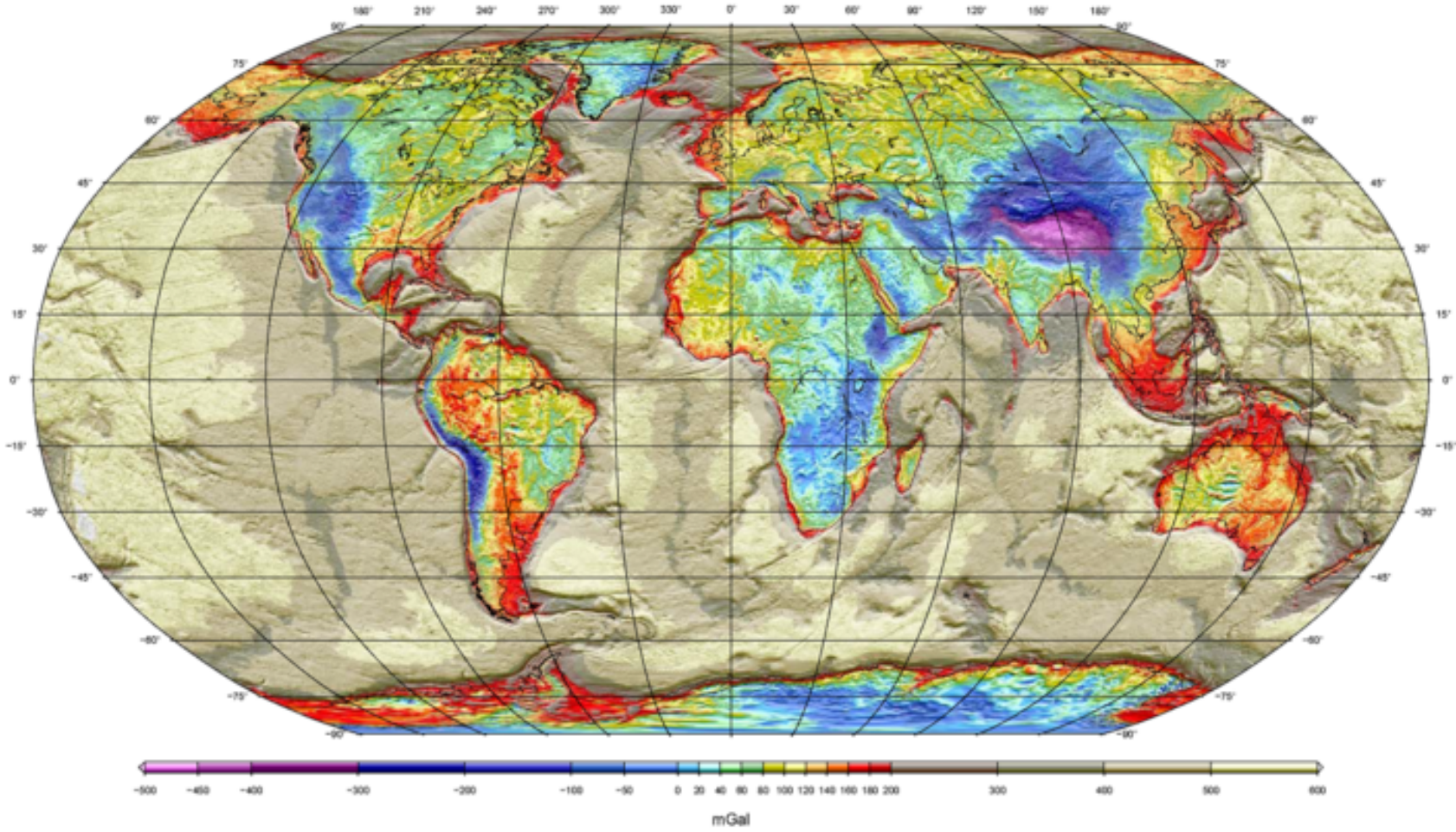

Geoid anomalies calculated wrt best fitting ellipsoid of revolution

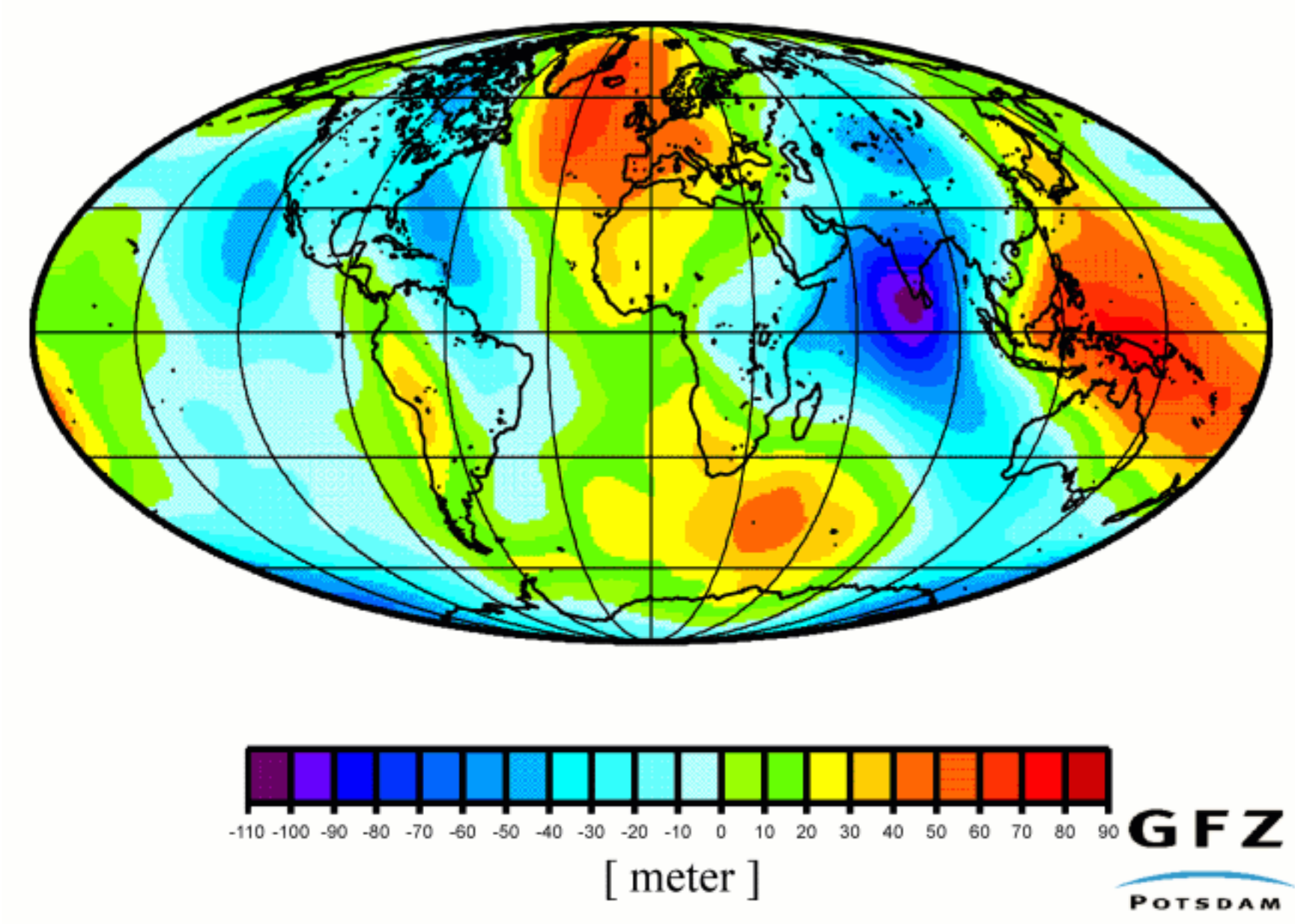

GOCE Geoid Anomaly Map in meters

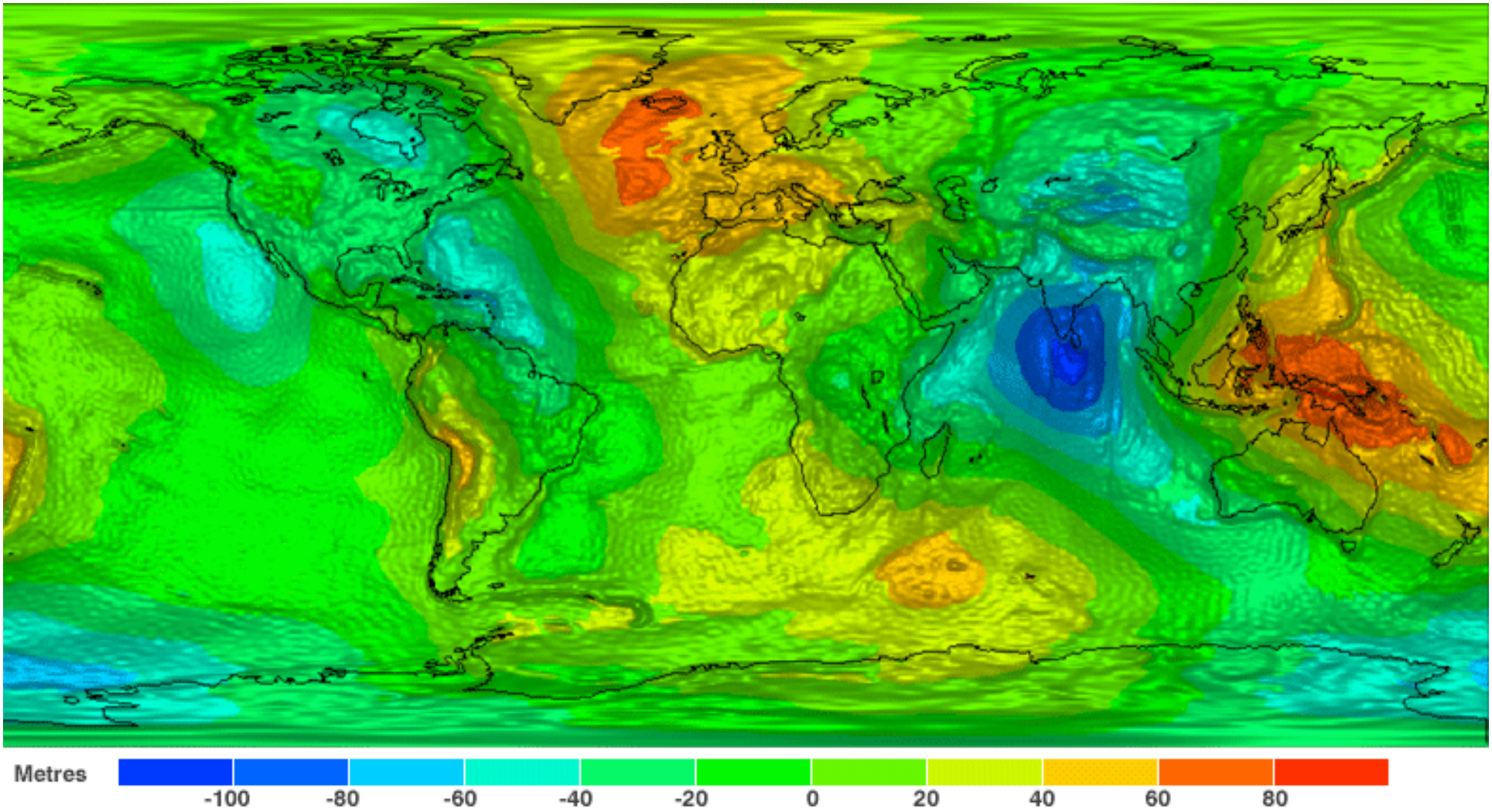

Geoid turned into gravity anomalies in mgals from GRACE

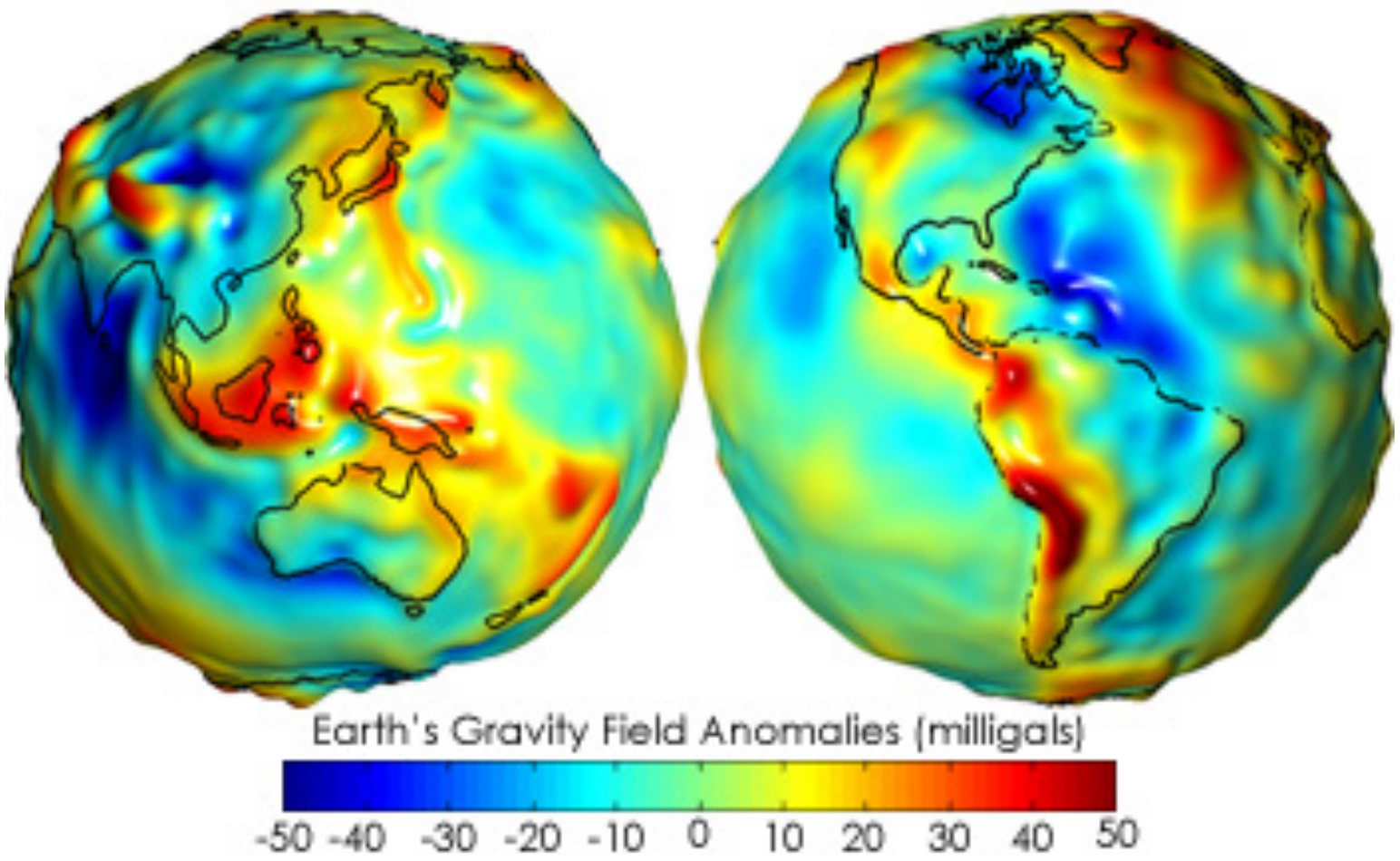

US Geoid: NASA/NOAA/National Geodetic Survey

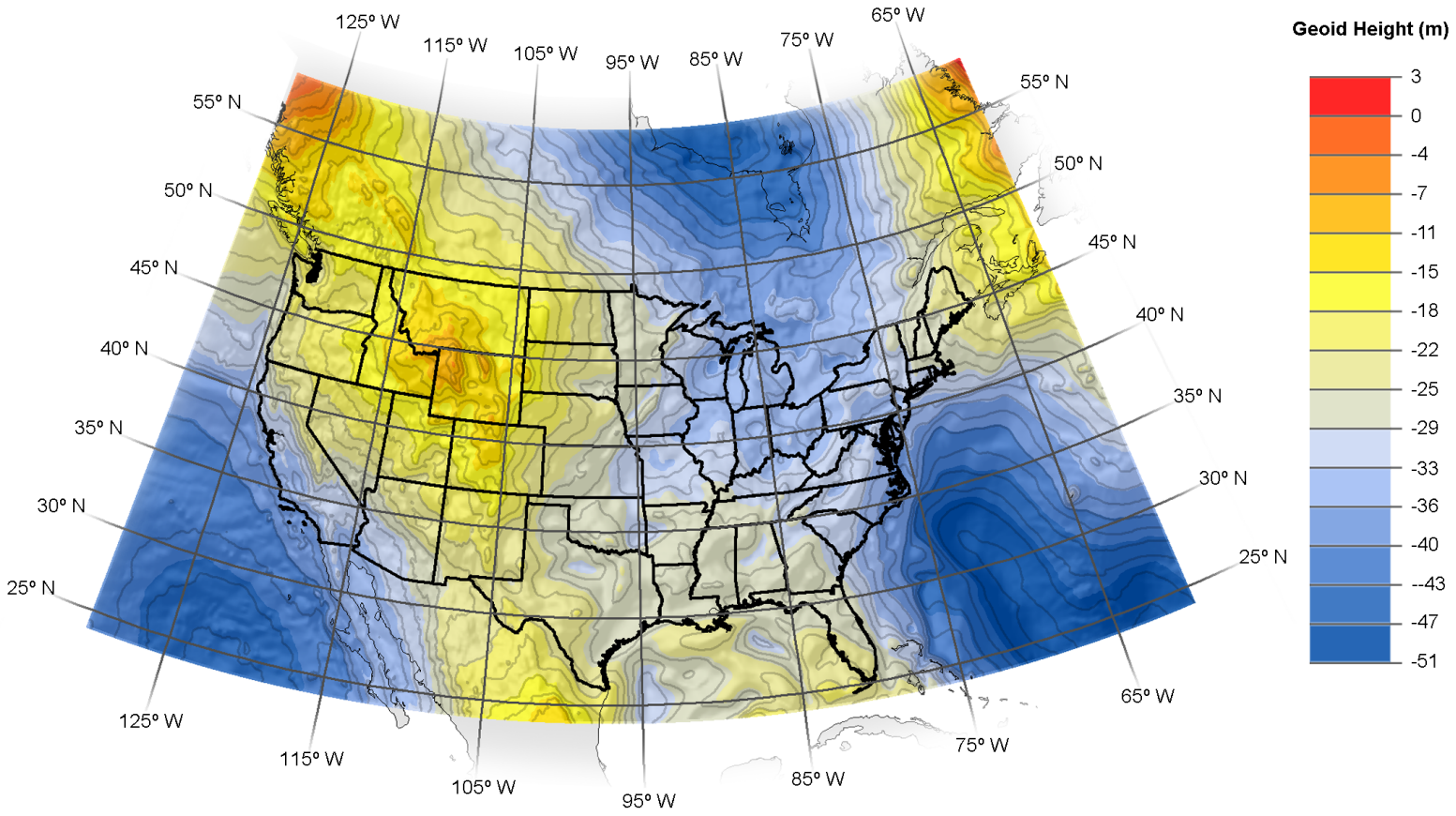

Notice the large positive anomaly in NW Wyoming. This is Yellowstone, a hotspot/plume.

What does this tell you about color bars?